Supporting information for:

2-Alkylphosphino-1-Boraadamantanes

Kurt F. Hoffmann[a], Rayni P. Noriega[a], Paul D. Boyle[a] and Marcus W. Drover[*a]

[a] Department of Chemistry, Western University, 1151 Richmond Street, London, ON, N8K 3G6, Canada.

marcus.drover@uwo.ca

Experimental Section:

General considerations. All experiments were carried out employing standard Schlenk techniques under an atmosphere of dry nitrogen employing degassed, dried solvents in a solvent purification system supplied by PPT, LLC. Non-halogenated solvents were tested with a standard purple solution of sodium benzophenone ketyl in tetrahydrofuran in order to confirm effective moisture removal. d_6-benzene was dried over molecular sieves and degassed by three freeze-pump-thaw cycles. All other reagents were purchased from commercial vendors and used without further purification unless otherwise stated. 3-Methoxy-7-(2-bromoethyl)-3-borabicyclo[3.3.1]non-6-ene (**5**), 2-(3-chloropropyl)-1-boraadamantane (**1**), 2-(2-chloroethyl)-1-boraadamantane (**3**), $LiPPh_2$, and $LiP(t\text{-}Bu)_2$ were prepared according to literature procedures.[1]

Physical methods. All NMR data were recorded with a Bruker AVIII HD 400 MHz or a Bruker Neo 600 MHz instrument. ^1H NMR spectra are reported in parts per million (ppm) and are referenced to residual solvent e.g., $^1H(C_6D_6)$: $\delta = 7.16$; $^{13}C(C_6D_6)$: $\delta = 128.06$; coupling constants are reported in Hz. ^{13}C, ^{31}P, and ^{11}B NMR spectra were performed as proton-decoupled experiments (unless explicitly stated otherwise) and are reported in ppm. Mass spectrometry was carried out with a Bruker micrOTOF 11 using electrospray ionization.

Preparation of Compounds:

General procedure for 2-alkylphosphine-1-boraadamantanes:

In the glovebox, the corresponding 2-chloroalkyl-1-boraadamantane was weighed into a 20 mL scintillation vial equipped with a stir bar and dissolved in 5 mL of THF and precooled to −35 °C. To this solution, the corresponding lithium phosphide dissolved in 10 mL of THF was added dropwise, which resulted in a rapid decolorization. After stirring the mixture for 1 h, all volatiles were removed *in vacuo*, resulting in a cloudy oil. The mixture was extracted with Et_2O, filtered and the filtrate subsequently dried in *vacuo*. The resulting solid was washed with cold *n*-pentane and dried again, yielding a colorless powder.

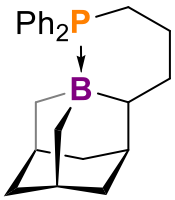

2-(3-diphenylphosphinopropyl)-1-boraadamantane (**2^{Ph}**; $C_{24}H_{30}BP$, 360 g/mol): 2-(3-chloropropyl)-1-boraadamantane (232 mg, 0.82 mmol) was reacted with $LiPPh_2$ (158 mg, 0.82 mmol, 1 equiv.) according to the general procedure described above. The resulting solid was washed with cold *n*-pentane and dried again, yielding a colorless powder (200 mg, 67%). Crystals suitable for X-ray diffraction were grown by cooling a concentrated solution in Et_2O to −35 °C overnight. **^{1}H NMR (600 MHz, d$_1$-CDCl$_3$, 298 K):** δ = 7.67 (m, 2H, -PPh_2), 7.45 (m, 8H, -PPh_2), 2.31 (m, 1H), 2.16 (m, 4H), 1.93 (m, 2H), 1.84 (m, 2H), 1.74 (m, 2H), 1.55 (m, 4H), 1.15 (m, 2H), 0.98 (m, 1H), 0.90 (m, 1H), 0.30 (m, 1H). **^{13}C{^{1}H} NMR (101 MHz, d$_1$-CDCl$_3$, 298 K):** δ = 133.7 (d, J = 8.7 Hz), 131.8 (d, J = 8.6 Hz), 130.6 (dd, J = 24.7, 2.3 Hz), 128.6 (dd, J = 9.0, 2.7 Hz), 41.9, 41.1 (d, J = 1.5 Hz), 38.2 (d, J = 11.7 Hz), 34.3, 32.2 – 31.5 (m), 23.7, 21.0 (d, J = 30.4 Hz). **^{31}P{^{1}H} NMR (243 MHz, d$_1$-CDCl$_3$, 298 K):** δ = −6.6. **^{11}B{^{1}H} NMR (193 MHz, d$_1$-CDCl$_3$, 298 K):** δ = −16.3. **HRESI(+)-MS:** calcd. 360.2173 exptl. 360.2125 for $C_{24}H_{30}BP$ $[M]^+$.

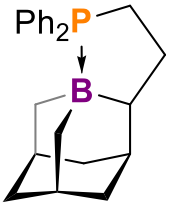

2-(2-diphenylphosphinoethyl)-1-boraadamantane (**4^{Ph}**; $C_{23}H_{28}BP$, 346 g/mol): 2-(2-chloroethyl)-1-boraadamantane (286 mg, 1.06 mmol) was reacted with $LiPPh_2$ (192 mg, 1.06 mmol, 1 equiv.) according to the general procedure described above. The resulting solid was washed with cold *n*-pentane and dried again, yielding a

colorless powder (333 mg, 91%). Crystals suitable for X-ray diffraction were grown by cooling a concentrated solution in Et_2O to −35 °C overnight. **^{1}H NMR (600 MHz, d_1-$CDCl_3$, 298 K):** δ = 7.45 (m, 10H, -PPh_2), 2.68 (m, 1H), 2.30 (m, 1H), 2.20 (m, 1H), 2.10 (m, 1H), 2.05 (m, 1H), 1.97 (m, 1H), 1.85 (m, 2H), 1.70 (m, 1H), 1.60 (m, 1H), 1.53 (m, 1H), 1.16 (m, 2H), 0.83 (m, 1H), 0.67 (m, 1H), 0.56 (m, 1H). **^{13}C{^{1}H} NMR (101 MHz, d_1-$CDCl_3$, 298 K):** δ = 132.5 (dd, J = 24.2, 9.4 Hz, -PPh_2), 130.4 (d, J = 9.8 Hz, -PPh_2), 128.7 (d, J = 9.4 Hz, -PPh_2), 41.1 (d, J = 30.0 Hz), 35.1 (d, J = 11.9 Hz), 33.8, 32.2 (d, J = 13.4 Hz), 27.7 (d, J = 10.2 Hz), 26.6 (d, J = 42.8 Hz). **^{31}P{^{1}H} NMR (243 MHz, d_1-$CDCl_3$, 298 K):** δ = 14.5. **^{11}B{^{1}H} NMR (193 MHz, d_1-$CDCl_3$, 298 K):** δ = −11.7. **HRESI(+)-MS:** calcd. 346.2016 exptl. 346.1966 for $C_{23}H_{28}BP$ $[M]^+$.

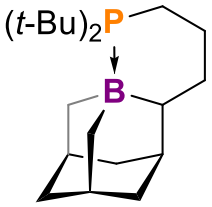

2-(3-di-*tert*-butylphosphinopropyl)-1-boraadamantane (**2$^{t\text{-Bu}}$**; $C_{20}H_{38}BP$, 320 g/mol): 2-(3-chloropropyl)-1-boraadamantane (292 mg, 1.03 mmol) was reacted with Li$P(t\text{-Bu})_2$ (157 mg, 1.03 mmol, 1 equiv.) according to the general procedure described above. The product was obtained as colorless crystals after recrystallization from Et_2O (180 mg, 55%). Crystals suitable for X-ray diffraction were grown by cooling a concentrated solution in Et_2O to −35 °C overnight. **^{1}H NMR (600 MHz, d_6-C_6D_6, 298 K):** δ = 2.56 (m, 2H), 2.27 (m, 1H), 2.21 (m, 1H), 2.11 (m, 3H), 2.03 (m, 1H), 1.94 (m, 1H), 1.85 (m, 1H), 1.78 (m, 1H), 1.60 (m, 1H), 1.50 (m, 1H), 1.40 (m, 1H), 1.33 (m, 3H), 1.27 (m, 2H), 1.10 (d, J = 11.0 Hz, 9H, -P(t-Bu)$_2$), 1.03 (m, 1H), 0.94 (d, J = 11.2 Hz, 9H, -P(t-Bu)$_2$). **^{13}C{^{1}H} NMR (101 MHz, d_6-C_6D_6, 298 K):** δ = 42.3, 41.6, 39.1 (d, J = 10.8 Hz), 34.4 (d, J = 4.5 Hz), 34.0 (m), 32.7 (d, J = 12.1 Hz), 32.4 (m), 30.1, 29.0, 24.8 (d, J = 2.2 Hz), 15.9 (d, J = 20.5 Hz). **^{31}P{^{1}H} NMR (243 MHz, d_6-C_6D_6, 298 K):** δ = 10.6. **^{11}B{^{1}H} NMR (193 MHz, d_6-C_6D_6, 298 K):** δ = −13.4. **HRESI(+)-MS:** calcd. 320.2799 exptl. 320.2741 for $C_{20}H_{38}BP$ $[M]^+$.

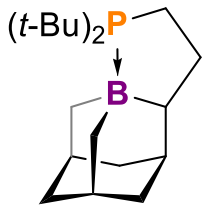

2-(2-di-*tert*-butylphosphinoethyl)-1-boraadamantane (**4$^{t\text{-Bu}}$**; $C_{19}H_{36}BP$, 306 g/mol): 2-(2-chloroethyl)-1-boraadamantane (325 mg, 1.21 mmol) was reacted with Li$P(t\text{-Bu})_2$ (184 mg, 1.21 mmol, 1 equiv.) according to the general procedure described above. The product was obtained as colorless crystals after recrystallization from Et_2O (254 mg, 69%). Crystals suitable for X-ray diffraction were grown by

cooling a concentrated solution in Et_2O to −35 °C overnight. **^{1}H NMR (600 MHz, d$_6$-C$_6$D$_6$, 298 K):** δ = 2.64 (m, 1H), 2.49 (m, 1H), 2.41 (m, 1H), 2.16 (m, 4H), 1.95 (m, 1H), 1.88 (m, 3H), 1.47 (m, 2H), 1.28 (m, 3H), 1.12 (m, 2H), 0.97 (dd, J = 11.7, 1.9 Hz, 18H, -P(t-Bu)$_2$). **^{13}C{^{1}H} NMR (101 MHz, d$_6$-C$_6$D$_6$, 298 K):** δ = 41.7 (d, J = 45.4 Hz), 35.6 (d, J = 10.4 Hz), 34.4, 33.2 (m), 29.9 (d, J = 2.6 Hz), 29.1 (d, J = 9.0 Hz), 28.9, 18.5 (d, J = 32.6 Hz). **^{31}P{^{1}H} NMR (243 MHz, d$_6$-C$_6$D$_6$, 298 K):** δ = 41.4. **^{11}B{^{1}H} NMR (193 MHz, d$_6$-C$_6$D$_6$, 298 K):** δ = −9.6. **HRESI(+)-MS:** calcd. 306.2642 exptl. 306.2637 for $C_{19}H_{36}BP$ $[M]^+$.

3-Methoxy-7-(2-diphenylphosphinoethyl)-3-borabicyclo[3.3.1]non-6-ene (**6^{Ph}**; $C_{23}H_{28}BOP$, 362 g/mol): In the glovebox, 3-methoxy-7-(2-bromoethyl)-3-borabicyclo[3.3.1]non-6-ene (507 mg, 1.97 mmol) was weighed into a 20 mL scintillation vial equipped with a stir bar and dissolved in 5 mL of THF and precooled to −35 °C. To this solution, LiP(t-Bu)$_2$ (379 mg, 1.97 mmol, 1 equiv.) dissolved in 10 mL of THF was added dropwise, which resulted in a rapid decolorization. After stirring the mixture for 2 h, all volatiles were removed *in vacuo*, resulting in a cloudy oil. The mixture was extracted with *n*-hexane, filtered and the filtrate subsequently dried in *vacuo*, yielding again a cloudy oil. The procedure was repeated until a colorless oil (661 mg, 92%) was obtained. **^{1}H NMR (600 MHz, d$_1$-CDCl$_3$, 298 K):** 7.42 (m, 10H, -PPh$_2$), 5.48 (m, 1H), 3.66 (s, 3H, -OMe), 2.47 (m, 2H), 2.35 (m, 1H), 2.14 (m, 2H), 2.03 (m, 2H), 1.78 (m, 1H), 1.66 (m, 2H), 1.09 (m, 1H), 1.00 (m, 1H), 0.88 (m, 1H). **^{13}C{^{1}H} NMR (101 MHz, d$_1$-CDCl$_3$, 298 K):** δ = 138.9 (t, J = 13.2 Hz), 134.1 (m), 132.8 (dd, J = 18.4, 11.1 Hz), 128.4 (m), 53.2, 37.5, 33.9 (d, J = 16.8 Hz), 32.7, 29.3, 27.5, 26.6 (d, J = 12.0 Hz), 25.0 (m). **^{31}P{^{1}H} NMR (243 MHz, d$_1$-CDCl$_3$, 298 K):** δ = −15.9. **^{11}B{^{1}H} NMR (193 MHz, d$_1$-CDCl$_3$, 298 K):** δ = 55.2.

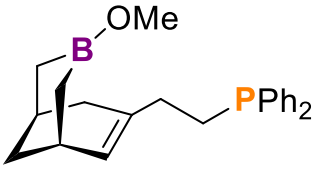

2-(1-di-phenylphosphinomethyl)-1-boraadamantane (**7^{Ph}**; $C_{26}H_{37}B_2OP$, 418 g/mol): 3-Methoxy-7-(2-diphenylphosphinoethyl)-3-borabicyclo[3.3.1]non-6-ene **6^{Ph}** (564 mg, 1.56 mmol) was dissolved in 10 mL THF in a Schlenk-flask equipped with a stir bar and a septum. The mixture was cooled to 0 °C and BH_3·THF (3.12 mL, 3.12 mmol, 2 eq.) was

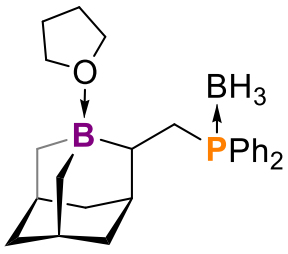

added dropwise via syringe. The septum is replaced by a reflux condenser and the reaction mixture was boiled under reflux conditions for 3 h. Subsequently, all volatiles were removed *in vacuo* and the residual solid was brought into a glovebox. There, the residue was washed three times with 5 mL of *n*-pentane each and further drying under reduced pressure yielded a colorless powder (530 mg, 81%). Crystals suitable for X-ray diffraction were grown by cooling a concentrated solution in THF to −35 °C overnight. **^{1}H NMR (600 MHz, d$_8$-THF, 298 K):** δ = 7.80 (m, 4H, -PPh$_2$), 7.42 (m, 6H, -PPh$_2$), 3.65 (m, 2H, THF), 2.64 (m, 1H), 2.14 (m, 2H), 2.01 (m, 1H), 1.81 (m, 2H, THF), 1.76 (m, 2H), 1.45 (m, 8H), 1.11 (m, 2H), 0.94 (m, 4H), 0.65 (m, 3H, -BH$_3$). **^{13}C{^{1}H} NMR (151 MHz, d$_8$-THF, 298 K):** δ = 132.6 (d, *J* = 8.8 Hz, -PPh$_2$), 131.9 (d, *J* = 8.2 Hz, -PPh$_2$), 130.2 (dd, *J* = 45.3, 2.4 Hz, -PPh$_2$), 128.2 (d, *J* = 9.3 Hz, -PPh$_2$), 128.0 (d, *J* = 9.4 Hz), 67.3 (THF), 40.3 (d, *J* = 16.0 Hz), 35.5 (d, *J* = 1.4 Hz), 33.3 (m), 25.4 (THF), 24.7 (d, *J* = 20.0 Hz), 24.5 (d, *J* = 3.6 Hz). **^{31}P{^{1}H} NMR (243 MHz, d$_8$-THF, 298 K):** δ = 16.4. **^{11}B{^{1}H} NMR (193 MHz, d$_8$-THF, 298 K):** δ = 10.6, −39.4 (-BH$_3$). **HRESI(+)-MS:** calcd. 387.2453 exptl. 387.2446 for C$_{24}$H$_{32}$B$_2$NP [M+CH$_3$CN (without THF)]$^+$.

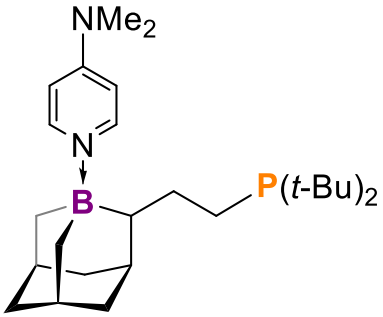

4-Dimethylaminopyridine adduct of 4$^{t\text{-Bu}}$ (8$^{t\text{-Bu}}$-DMAP; C$_{26}$H$_{46}$BN$_2$P, 428 g/mol): 2-(2-di-*tert*-butylphosphinoethyl)-1-boraadamantane **4$^{t\text{-Bu}}$** (18 mg, 0.06 mmol) was weighed into a 20 mL scintillation vial equipped with a stir bar and dissolved in 2 mL of toluene. To this solution, 4-dimethylaminopyridine (7 mg, 0.06 mmol, 1 eq.) dissolved in 2 mL of toluene was added. After stirring the mixture for 10 mins, all volatiles were removed *in vacuo* and the oily residue washed with 2 mL of cold pentane. Further drying with reduced pressure resulted in a colorless powder (23 mg, 90%). Crystals suitable for X-ray diffraction were grown by slowly evaporating a solution in *n*-pentane overnight. **^{1}H NMR (600 MHz, d$_6$-C$_6$D$_6$, 298 K):** δ = 7.94 (m, 2H, DMAP), 5.58 (m, 2H, DMAP), 2.89 (m, 2H), 2.68 (m, 1H), 2.43 (m, 1H), 2.33 (m, 2H), 2.27 (m, 1H), 2.21 (m, 2H), 1.99 (m, 2H), 1.94 (s, 6H, -NMe$_2$), 1.77 (m, 1H), 1.48 (m, 1H), 1.31 (m, 2H), 1.20 (m, 2H), 1.11 (m, 1H), 1.11 (dd, *J* = 48.1, 10.3 Hz, 18H, -P(*t*-Bu)$_2$). **^{13}C{^{1}H} NMR (101 MHz, d$_6$-C$_6$D$_6$, 298 K):** δ = 153.8 (m, DMAP), 143.4 (DMAP), 105.9 (DMAP), 42.6, 41.6, 37.8 (DMAP), 35.3, 34.6, 33.7, 33.2, 31.3 (d, *J* = 23.4 Hz), 30.9 (dd, *J* = 28.8, 23.8

Hz), 29.7 (t, J = 13.6 Hz), 21.5 (d, J = 21.8 Hz). **^{31}P{^{1}H} NMR (243 MHz, d$_6$-C$_6$D$_6$, 298 K):** δ = 28.8. **^{11}B{^{1}H} NMR (193 MHz, d$_6$-C$_6$D$_6$, 298 K):** δ = −4.6. **HRESI(+)-MS:** calcd. 429.3564 exptl. 429.3565 for $C_{26}H_{47}BN_2P$ $[M+H]^+$.

Reaction of 4$^{t\text{-Bu}}$ with HNEt$_2$ (8$^{t\text{-Bu}}$-HNEt$_2$; $C_{23}H_{47}BNP$, 379 g/mol): 2-(2-di-*tert*-butylphosphinoethyl)-1-boraadamantane **4$^{t\text{-Bu}}$** (10 mg, 0.032 mmol) was weighed into a 20 mL scintillation vial equipped with a stir bar and dissolved in 500 µL of C_6D_6. To this solution, $HNEt_2$ (3.31 µL, 0.032 mmol, 1 eq.) was added, giving a pale-yellow solution after 5 mins, that was characterized as a 1:0.37 mixture of **4$^{t\text{-Bu}}$:8$^{t\text{-Bu}}$-HNEt$_2$**. Addition of excess $HNEt_2$ (86 µL, 0.83 mmol, 26 eq.) to **4$^{t\text{-Bu}}$** (10 mg, 0.032 mmol) provides a 1:5.7 mixture of **4$^{t\text{-Bu}}$:8$^{t\text{-Bu}}$-HNEt$_2$**. Upon application of vacuum, exclusive formation of ring-closed **4$^{t\text{-Bu}}$** is observed, confirming $HNEt_2$ lability. **^{1}H NMR (600 MHz, d$_6$-C$_6$D$_6$, 298 K, select signals):** δ = 3.65 (m, 1H, CH($HNEt_2$)), 3.43 (m, 1H, CH($HNEt_2$)), 2.02 (m, 2H, CH($HNEt_2$) by ^{1}H-^{1}H COSY), 1.23 (m, 6H, CH_3($HNEt_2$) by ^{1}H-^{1}H COSY). Free $HNEt_2$: (δ = 2.47 (4H, q, $^{3}J_{H,H}$ = 7.3 Hz), 0.99 (6H, t, $^{3}J_{H,H}$ = 7.3 Hz). **^{31}P{^{1}H} NMR (243 MHz, d$_6$-C$_6$D$_6$, 298 K):** δ = 41.4 (**4$^{t\text{-Bu}}$**), 29.5 (**8$^{t\text{-Bu}}$-HNEt$_2$**). **^{11}B{^{1}H} NMR (193 MHz, d$_6$-C$_6$D$_6$, 298 K):** δ = −4.0 (**8$^{t\text{-Bu}}$-HNEt$_2$**), −9.6 (**4$^{t\text{-Bu}}$**). **HRESI(+)-MS:** calcd. 307.2726 exptl. 307.2720 for $C_{19}H_{37}BP$ $[M+H\text{-}HNEt_2]^+$.

Gold complex of 8$^{t\text{-Bu}}$-DMAP (**9$^{t\text{-Bu}}$**; $C_{26}H_{46}AuBClN_2P$, 660 g/mol):

[$AuCl(SMe_2)$] (20 mg, 0.07 mmol) was weighed into a 20 mL scintillation vial equipped with a stir bar and dissolved in 2 mL of *ortho*-difluorobenzene. To this solution, freshly prepared **8$^{t\text{-Bu}}$-DMAP** (29 mg, 0.07 mmol, 1 eq.) dissolved in 2 mL of *ortho*-difluorobenzene was added. After stirring the mixture for 2 h, a dark precipitate has formed and the mixture was filtered through celite, resulting in a clear, colorless solution. All volatiles were removed *in vacuo* and the residue subsequently washed with 2 x 2 mL of cold pentane. Further drying with reduced pressure resulted in a colorless powder (36 mg, 78%).

Crystals suitable for X-ray diffraction were grown by cooling down a concentrated solution in Et_2O to −35 °C overnight. **^{1}H NMR (600 MHz, d$_6$-C$_6$D$_6$, 298 K):** δ = 8.01 (m, 2H, DMAP), 6.11 (m, 2H, DMAP), 2.85 (m, 2H), 2.43 (m, 1H), 2.37 (m, 1H), 2.28 (s, 6H, DMAP), 2.23 (m, 3H), 2.09 (m, 1H), 1.99 (m, 1H), 1.94 (m, 2H), 1.88 (m, 1H), 1.43 (m, 2H), 1.34 (m, 1H), 1.23 (m, 2H), 1.09 (m, 2H), 0.86 (d, J = 14.4 Hz, 9H, -P(t-Bu)$_2$), 0.76 (d, J = 14.4 Hz, 9H, -P(t-Bu)$_2$). **^{13}C{^{1}H} NMR (101 MHz, d$_6$-C$_6$D$_6$, 298 K):** δ = 154.4, 142.9, 106.9, 42.3, 41.3, 38.3, 34.4 (m), 33.5, 32.9, 31.4 (d, J = 1.6 Hz), 29.1 (d, J = 4.8 Hz), 28.7 (d, J = 4.9 Hz), 20.4 (d, J = 26.2 Hz). **^{31}P{^{1}H} NMR (243 MHz, d$_6$-C$_6$D$_6$, 298 K):** δ = 75.1. **^{11}B{^{1}H} NMR (193 MHz, d$_6$-C$_6$D$_6$, 298 K):** δ = −5.4. **HRESI(+)-MS:** calcd. 660.2840 exptl. 660.2828 for $C_{26}H_{46}AuBClN_2P$ $[M]^+$.

Platinum complex of 8$^{t\text{-Bu}}$-DMAP (**10$^{t\text{-Bu}}$**; $C_{54}H_{98}B_2N_4P_2Pt$, 1082 g/mol): [Pt(Me)$_2$(COD)] (20 mg, 0.06 mmol) was weighed into a 25 mL Schlenk bomb equipped with a stir bar and dissolved in 2 mL of toluene. To this solution, freshly prepared **8$^{t\text{-Bu}}$-DMAP** (50 mg, 0.12 mmol, 2 eq.) dissolved in 10 mL of toluene was added. Subsequently, the mixture was heated to 80 °C for 16 h which led to the precipitation of a colorless solid. The supernatant was decanted and the remaining solid washed with 2 x 2 mL of n-pentane. Further drying with reduced pressure resulted in a colorless powder (23 mg, 35%). Crystals suitable for X-ray diffraction were grown by vapor diffusion of n-hexane onto a concentrated solution in THF over 3 days. **^{1}H NMR (600 MHz, d$_8$-THF, 298 K):** δ = 8.02 (m, 4H, DMAP), 6.70 (m, 4H, DMAP), 3.11 (s, 12H, DMAP), 2.19 (m, 4H), 2.07 (m, 3H), 1.81 (m, 4H), 1.62 (m, 6H), 1.41 (d, J = 12.4 Hz, 4H), 1.36 – 1.13 (br, 43H, -P(t-Bu)$_2$), 0.93 (m, 2H), 0.77 (s, 4H), 0.58 (m, 3H), -0.18 (br, 5H). **^{13}C{^{1}H} NMR (101 MHz, d$_8$-THF, 298 K):** δ = 155.0, 143.4, 106.5, 66.3, 42.1, 41.0, 38.3, 34.7, 33.2, 32.8, 31.5, 30.7, 30.2, 24.3, 22.5, 13.4. **^{31}P{^{1}H} NMR (243 MHz, d$_8$-THF, 298 K):** δ = 33.8 ($^1J(^{195}Pt,^{31}P)$ = 3012 Hz). **^{11}B{^{1}H} NMR (193 MHz, d$_8$-THF, 298 K):** δ = −4.7. **HRESI(+)-MS:** calcd. 1066,6865 exptl. 1066.6876 for $C_{53}H_{95}B_2N_4P_2Pt$ $[M\text{-}CH_3]^+$.

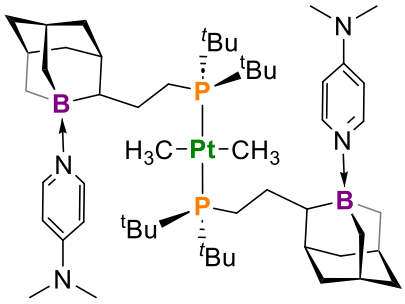

Multinuclear NMR Data:

Figure S1: 2^{Ph}, ^{1}H NMR, d$_1$-CDCl$_3$, 600 MHz, 298 K.

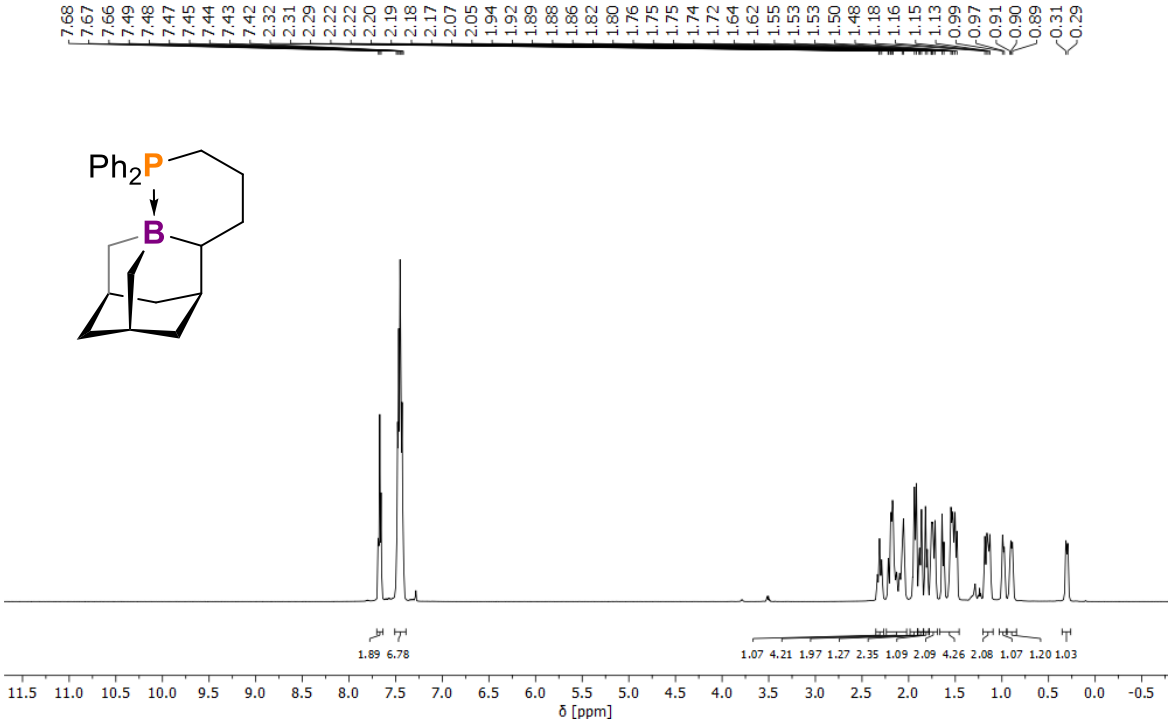

Figure S2: 2^{Ph}, ^{31}P{^{1}H} NMR, d$_1$-CDCl$_3$, 243 MHz, 298 K.

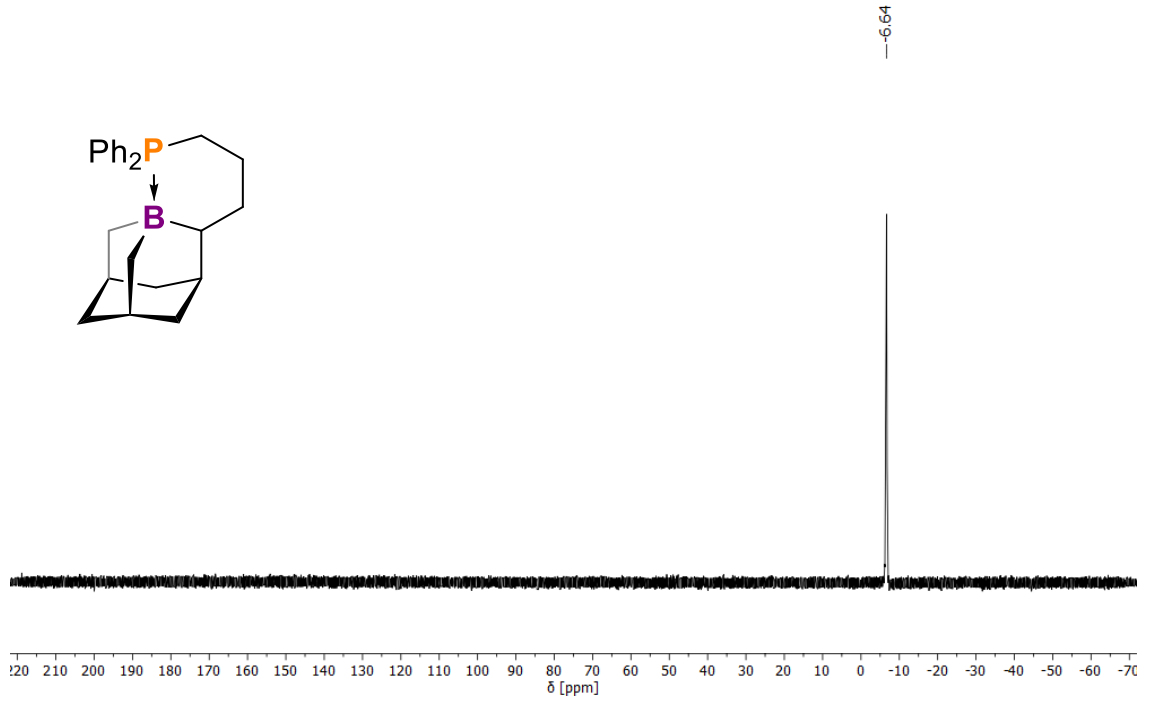

Figure S3: 2^{Ph}, $^{11}B\{^{1}H\}$ NMR, d_1-$CDCl_3$. 193 MHz, 298 K.

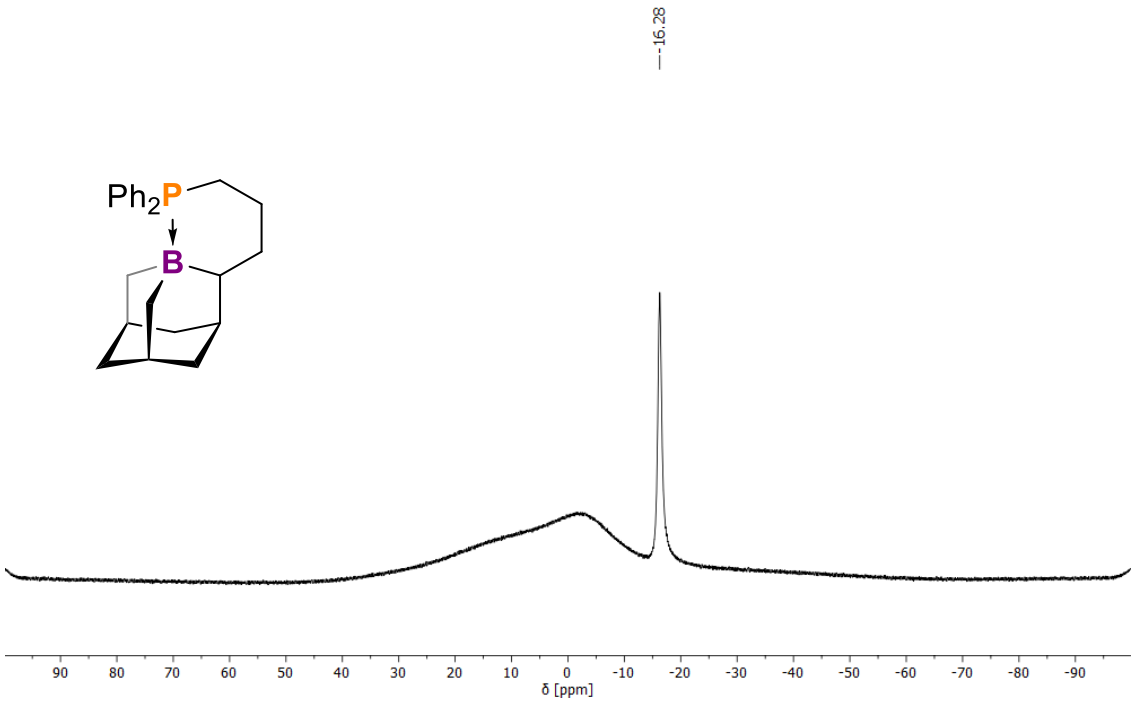

Figure S4: 2^{Ph}, $^{13}C\{^{1}H\}$ NMR, d_1-$CDCl_3$, 101 MHz, 298 K.

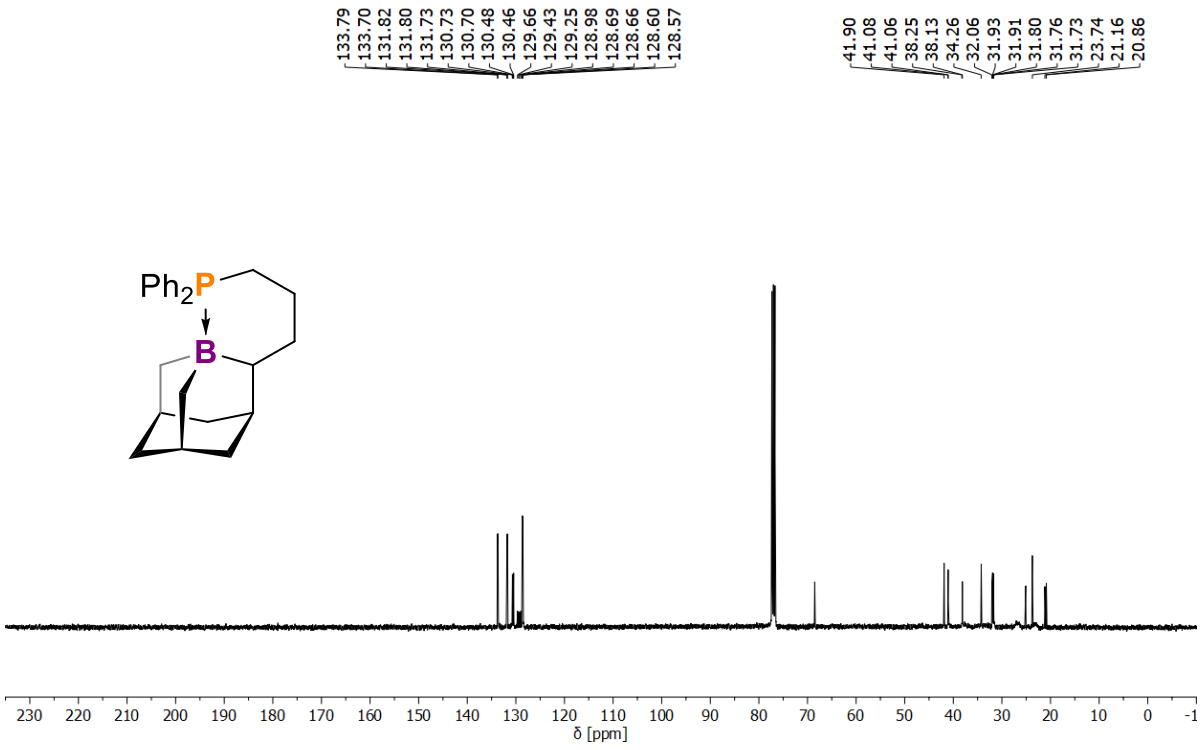

Figure S5: 4^{Ph}, ^{1}H NMR, d$_1$-CDCl$_3$, 600 MHz, 298 K.

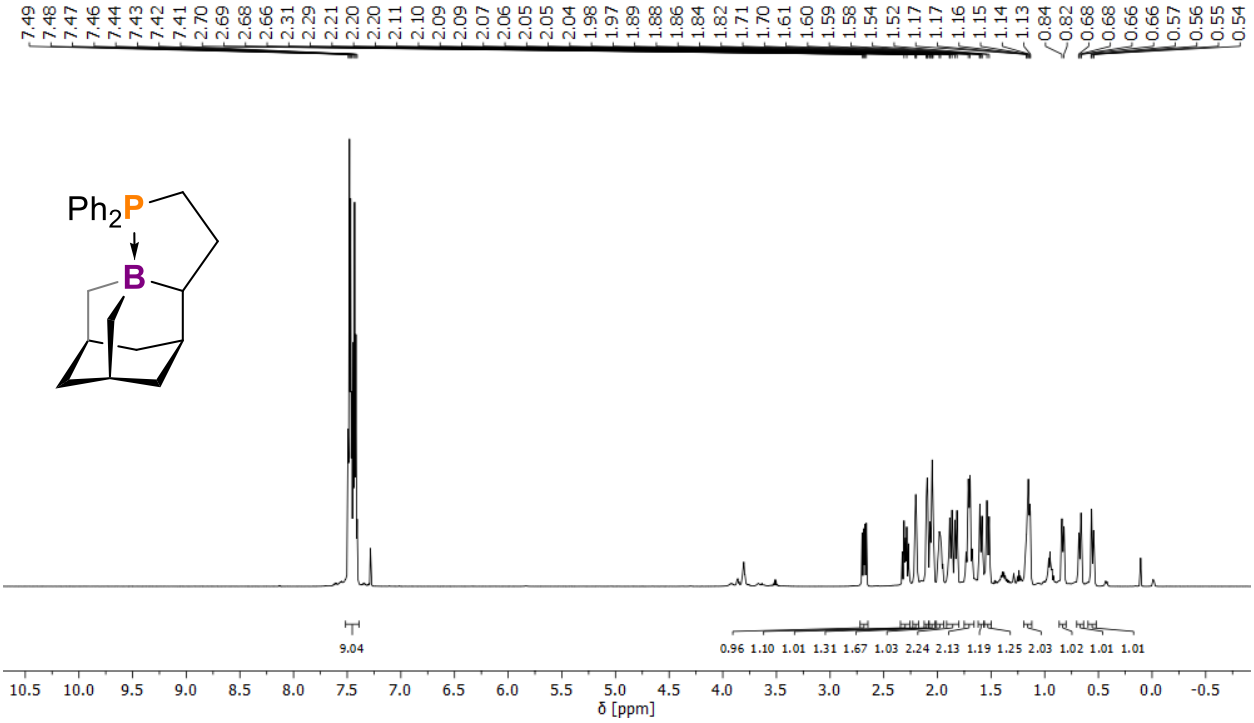

Figure S6: 4^{Ph}, ^{31}P{^{1}H} NMR, d$_1$-CDCl$_3$, 243 MHz, 298 K.

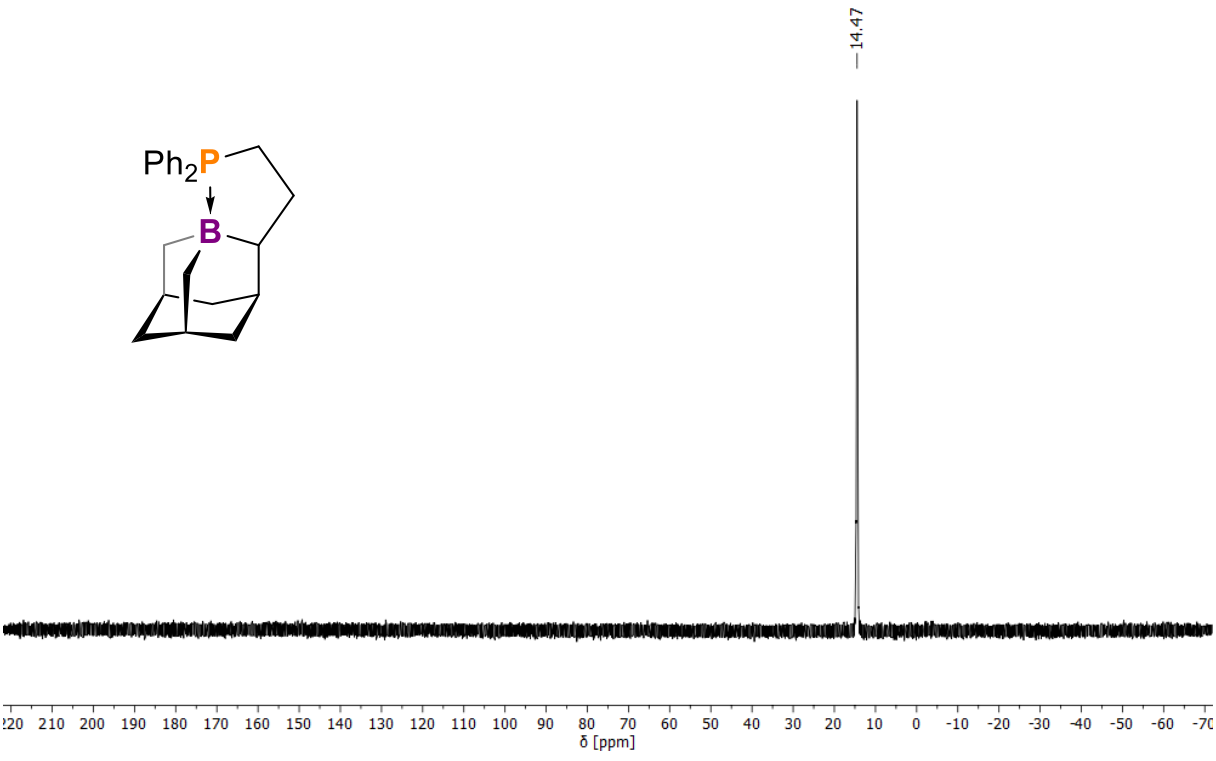

Figure S7: 4^{Ph}, $^{11}B\{^{1}H\}$ NMR, d_1-$CDCl_3$. 193 MHz, 298 K.

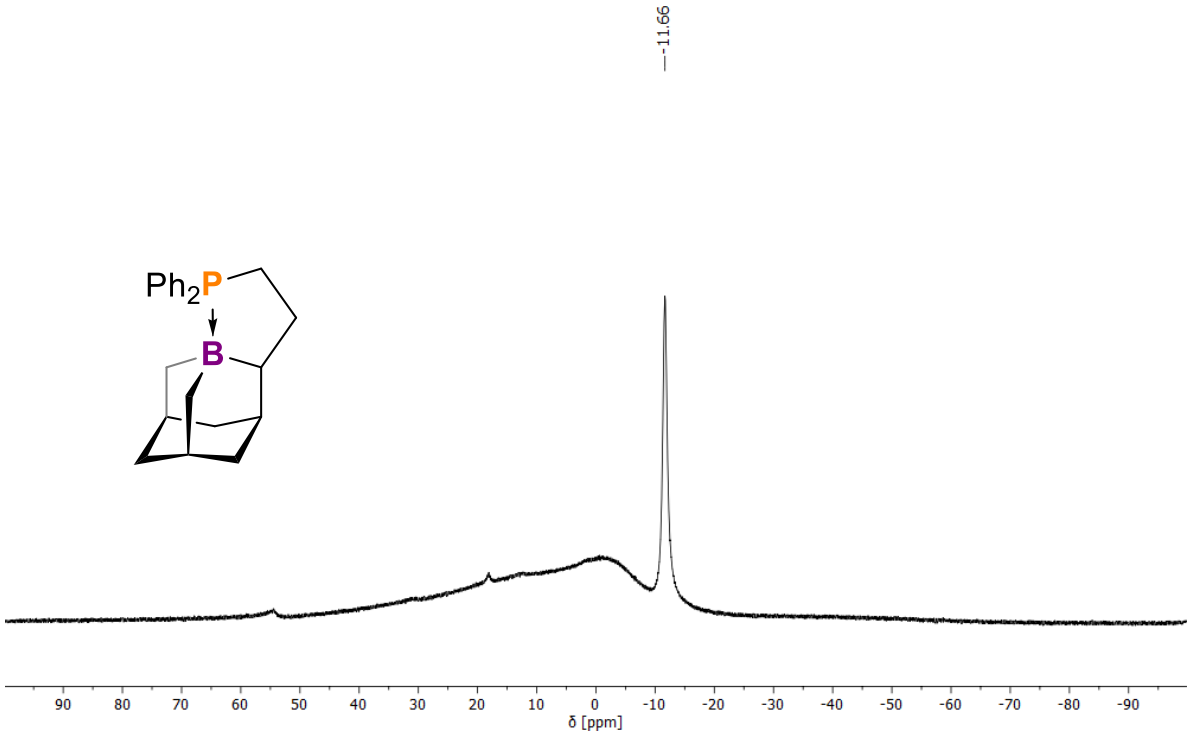

Figure S8: 4^{Ph}, $^{13}C\{^{1}H\}$ NMR, d_1-$CDCl_3$, 101 MHz, 298 K.

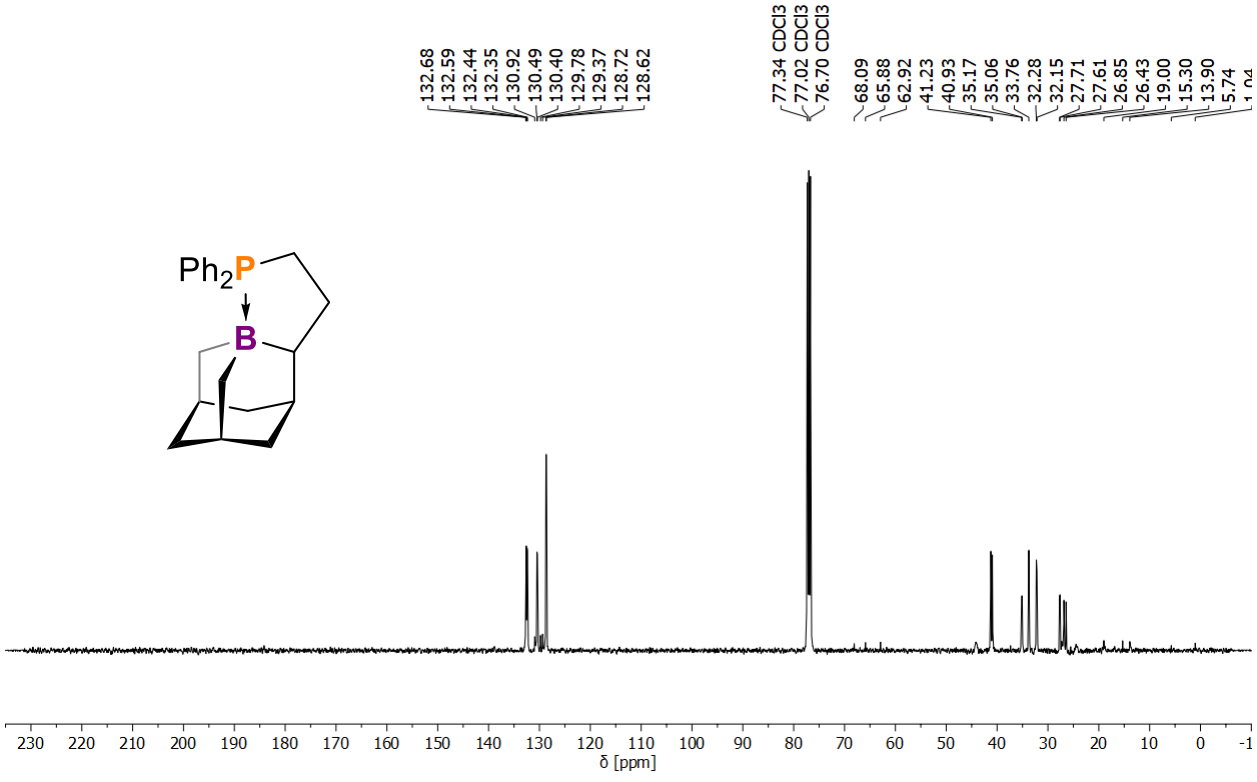

Figure S9: 2$^{t\text{-Bu}}$, ^{1}H NMR, d$_6$-C$_6$D$_6$, 600 MHz, 298 K. * denotes traces of THF.

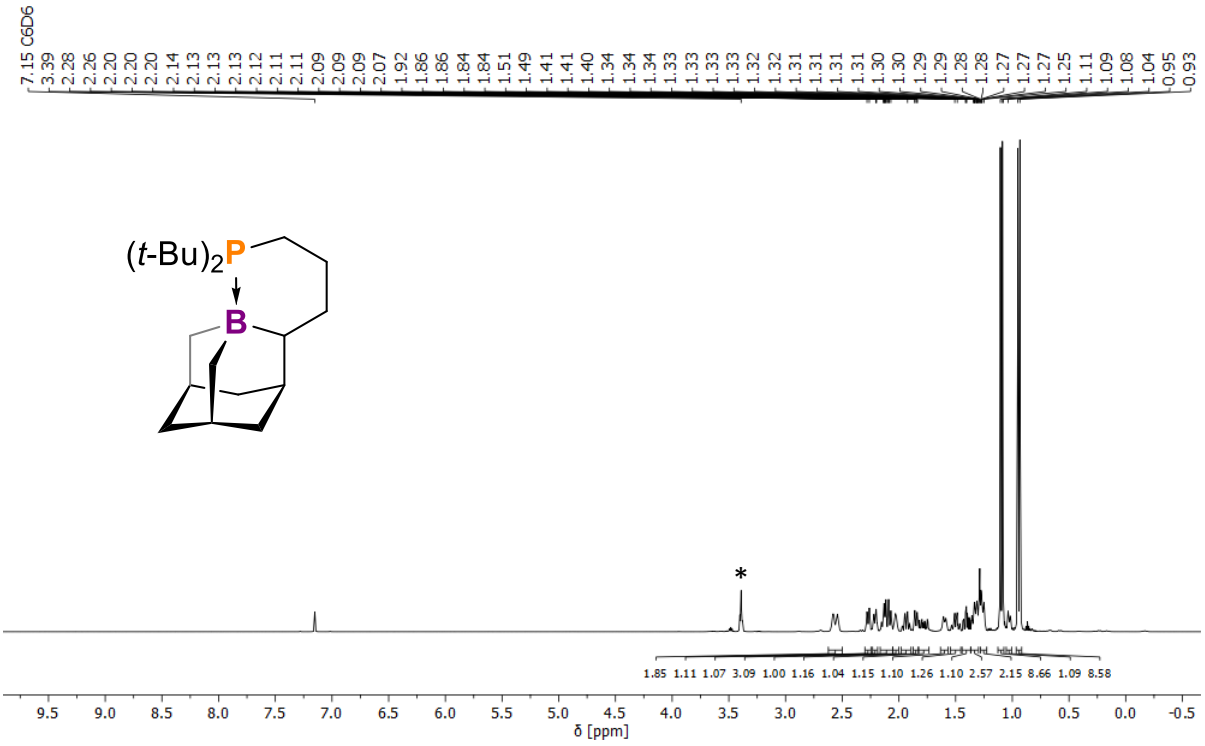

Figure S10: 2$^{t\text{-Bu}}$, ^{31}P{^{1}H} NMR, d$_6$-C$_6$D$_6$, 243 MHz, 298 K.

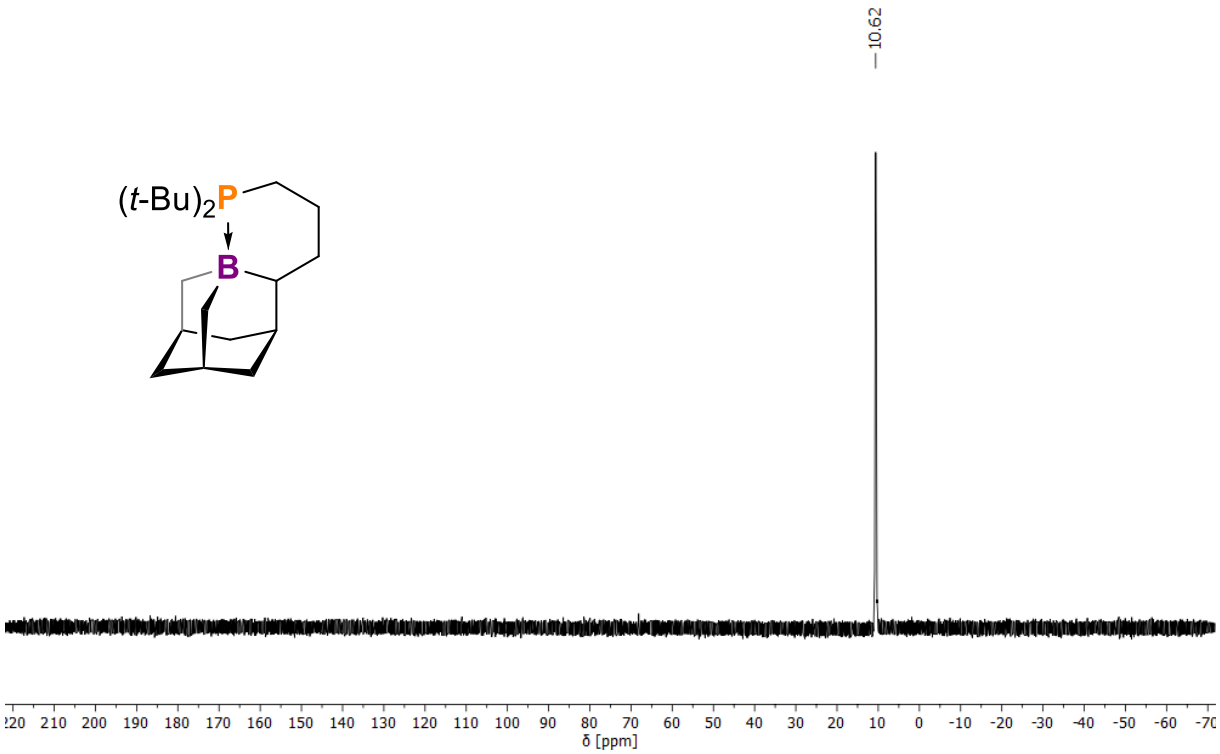

Figure S11: 2$^{t\text{-Bu}}$, $^{11}B\{^{1}H\}$ NMR, d$_6$-C$_6$D$_6$, 193 MHz, 298 K. * denotes unknown impurity.

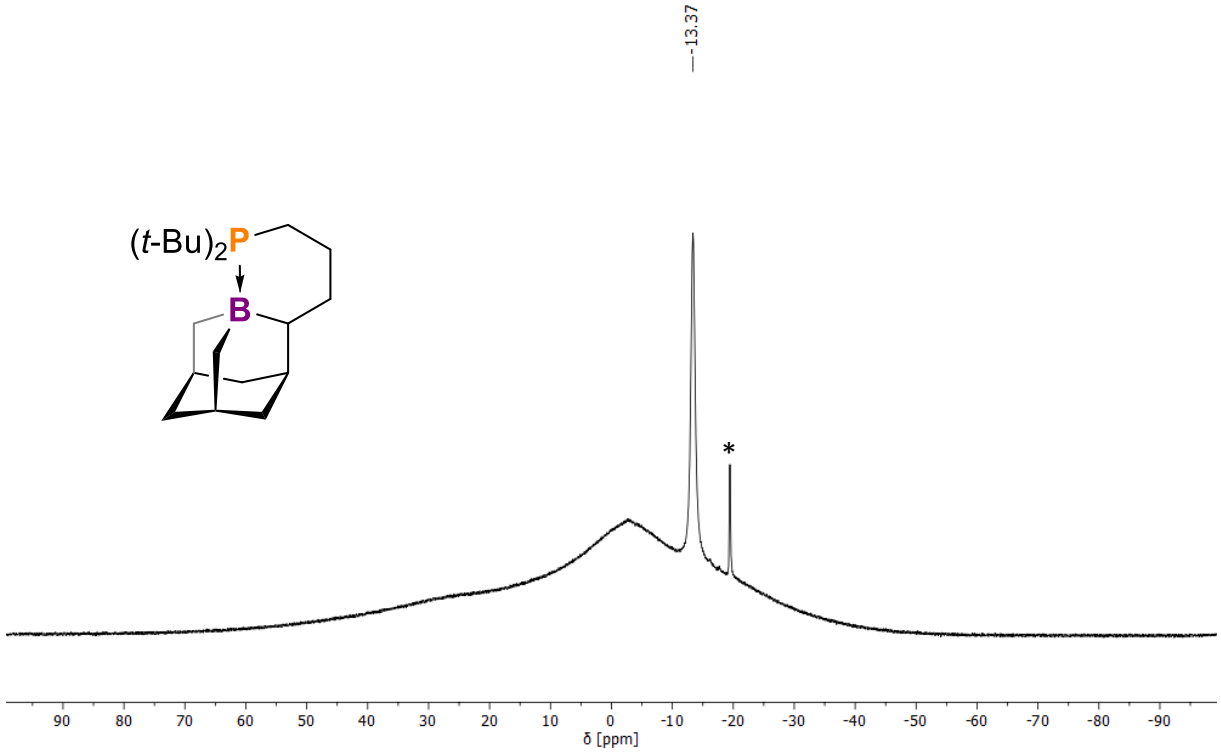

Figure S12: 2$^{t\text{-Bu}}$, $^{13}C\{^{1}H\}$ NMR, d$_6$-C$_6$D$_6$, 101 MHz, 298 K. * denotes traces of THF.

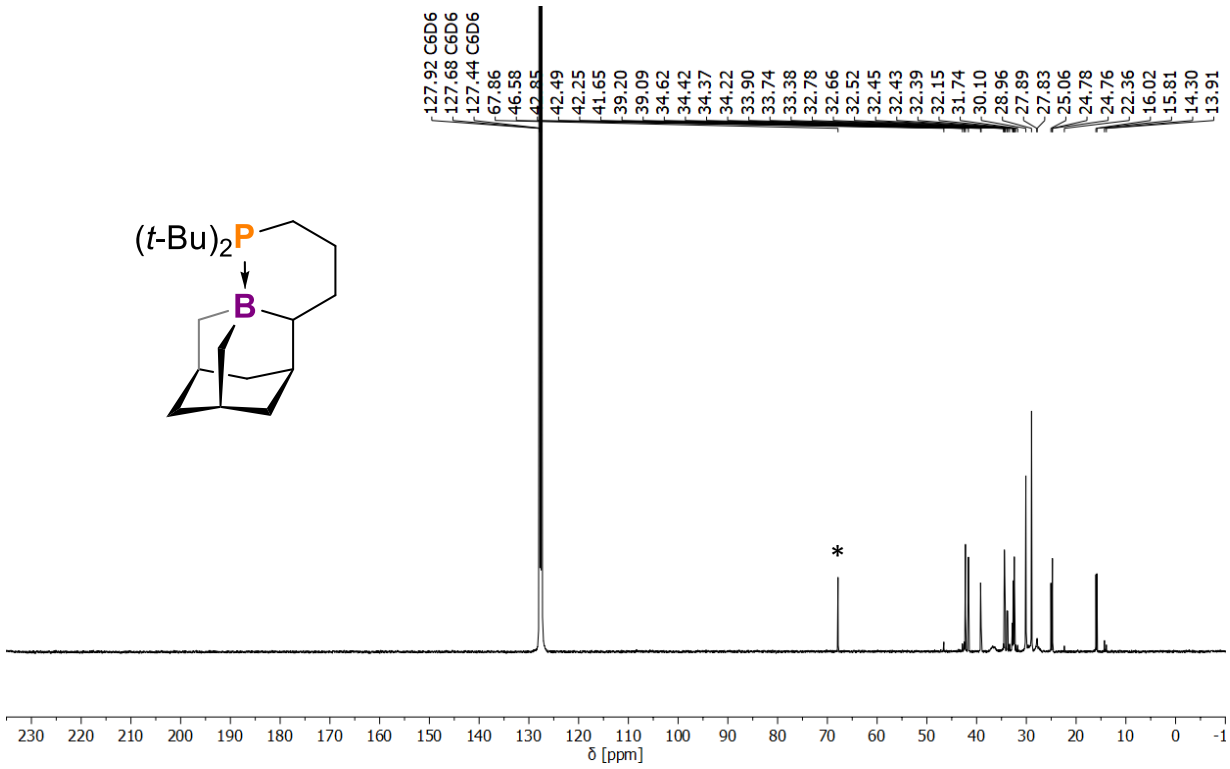

Figure S13: 4$^{t\text{-Bu}}$, ^{1}H NMR, d$_6$-C$_6$D$_6$, 600 MHz, 298 K. * denotes traces of THF.

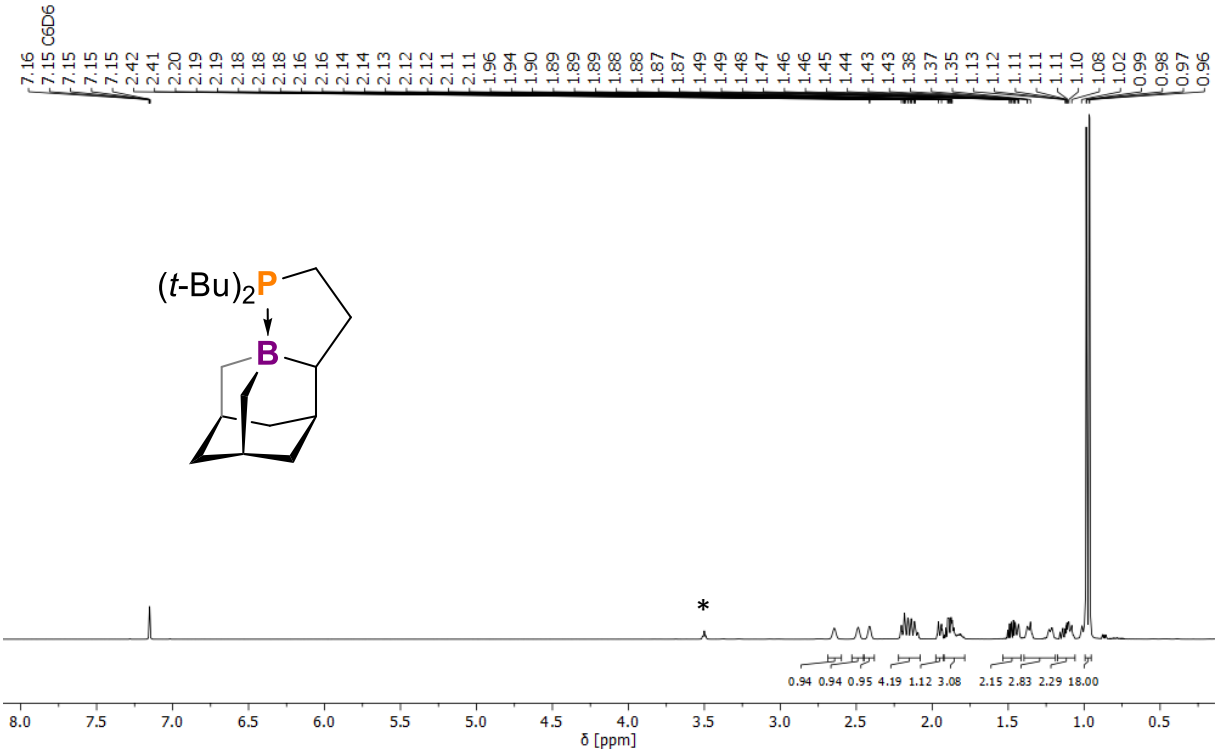

Figure S14: 4$^{t\text{-Bu}}$, ^{31}P{^{1}H} NMR, d$_6$-C$_6$D$_6$, 243 MHz, 298 K.

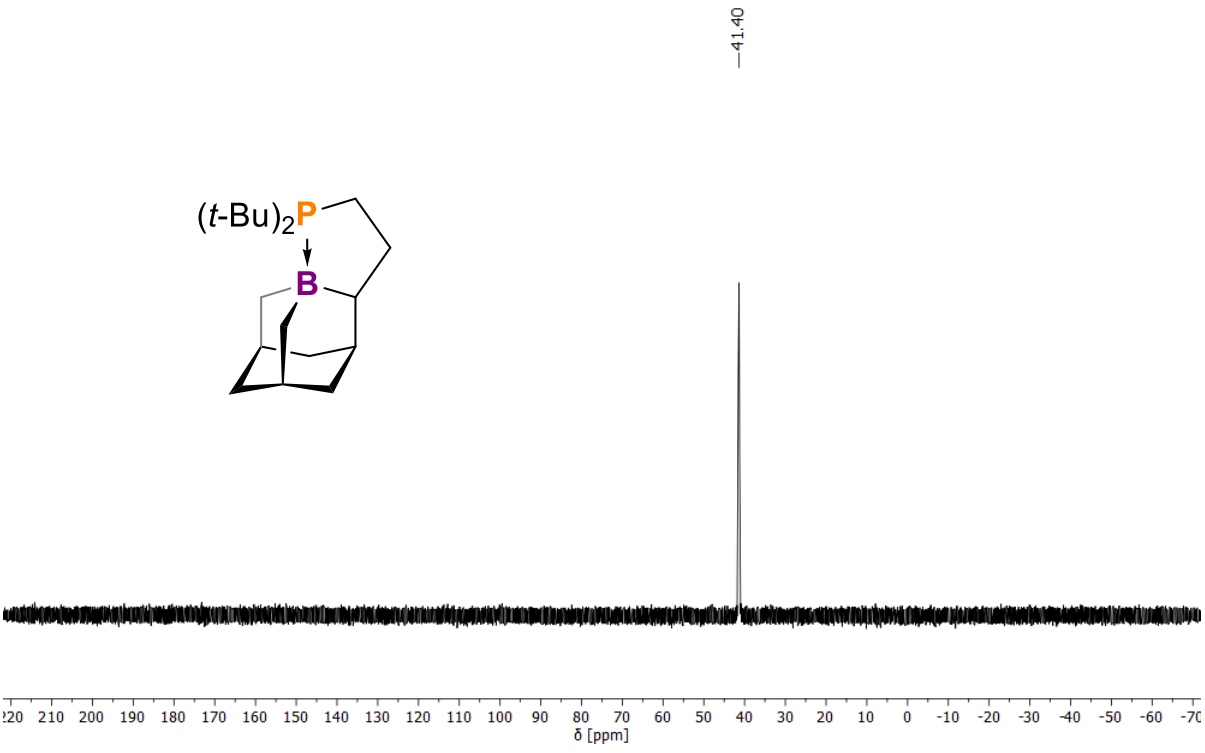

Figure S15: 4$^{t\text{-Bu}}$, $^{11}B\{^{1}H\}$ NMR, d_6-C_6D_6. 193 MHz, 298 K. * denotes unknown impurity.

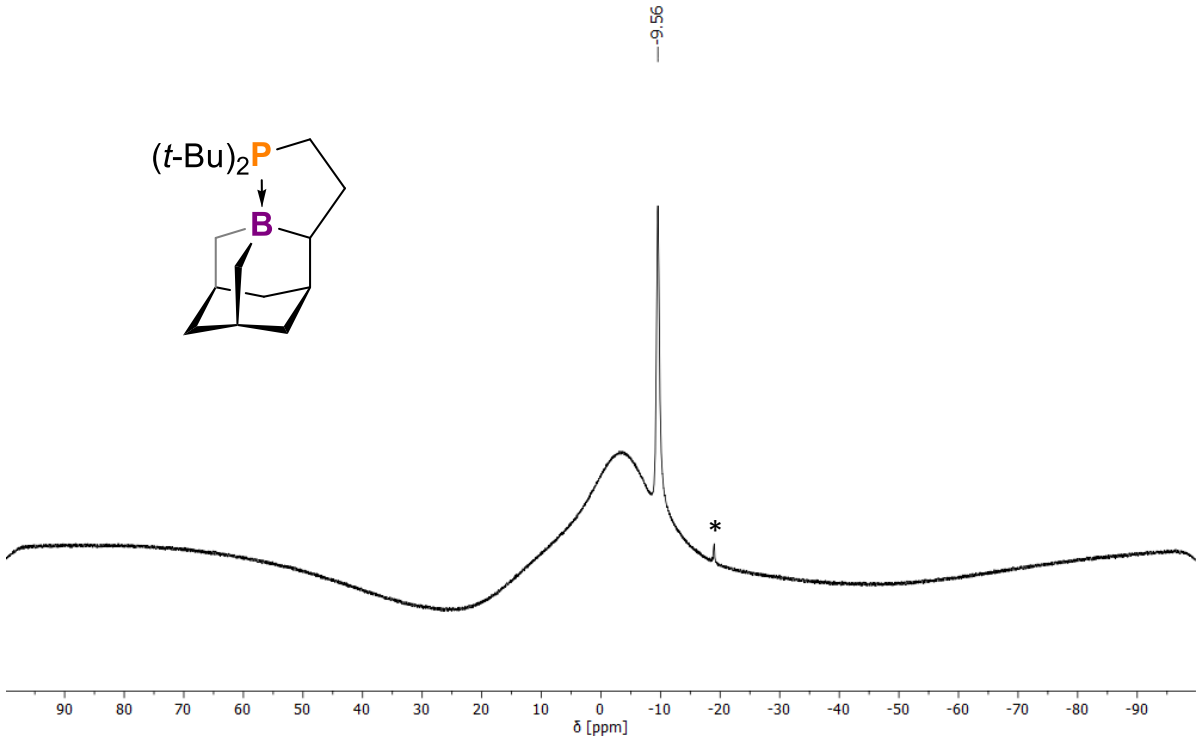

Figure S16: 4$^{t\text{-Bu}}$, $^{13}C\{^{1}H\}$ NMR, d_6-C_6D_6, 101 MHz, 298 K. * denotes traces of THF.

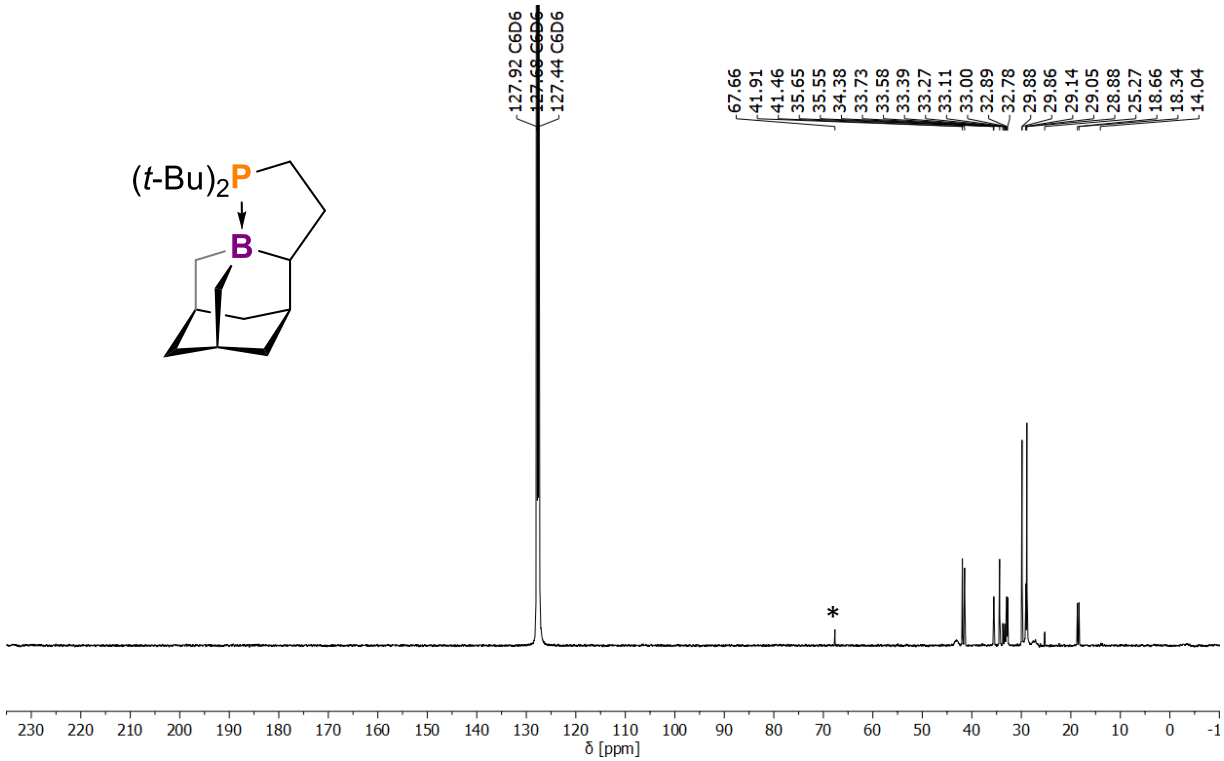

Figure S17: 6^{Ph}, ^{1}H NMR, d$_1$-CDCl$_3$, 600 MHz, 298 K. * denotes residual *n*-pentane.

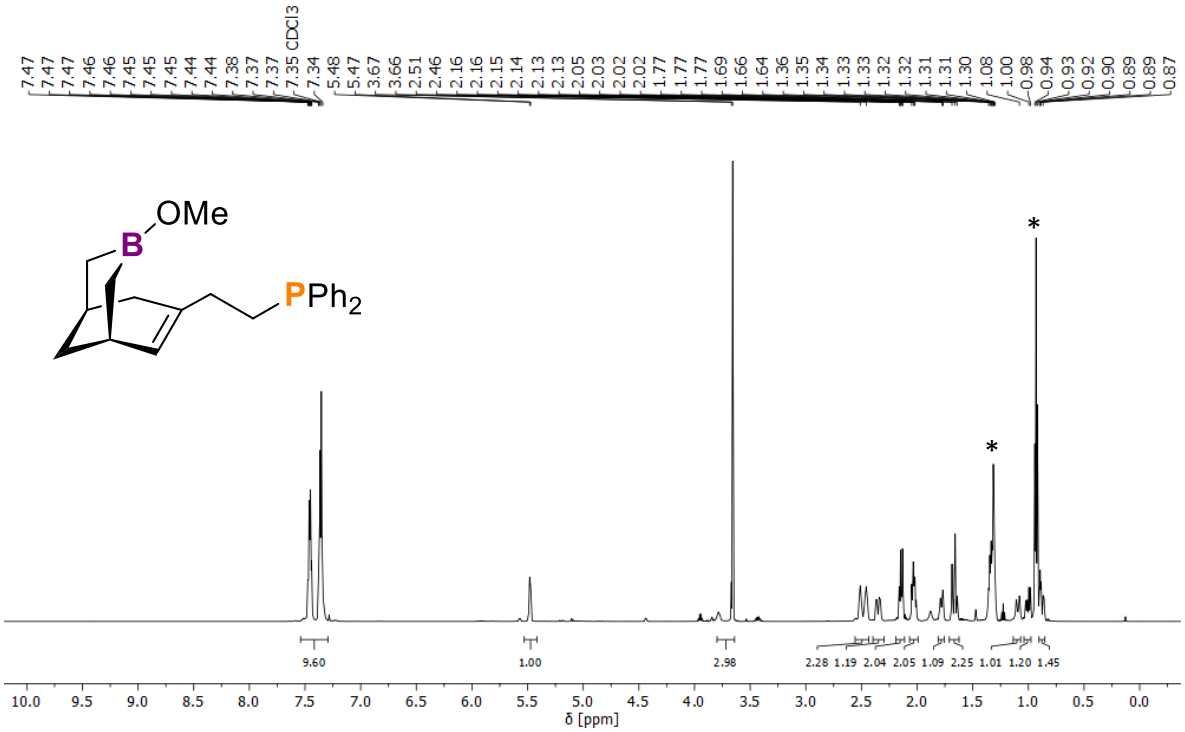

Figure S18: 6^{Ph}, ^{31}P{^{1}H} NMR, d$_1$-CDCl$_3$, 243 MHz, 298 K. * denotes trace HPPh$_2$.

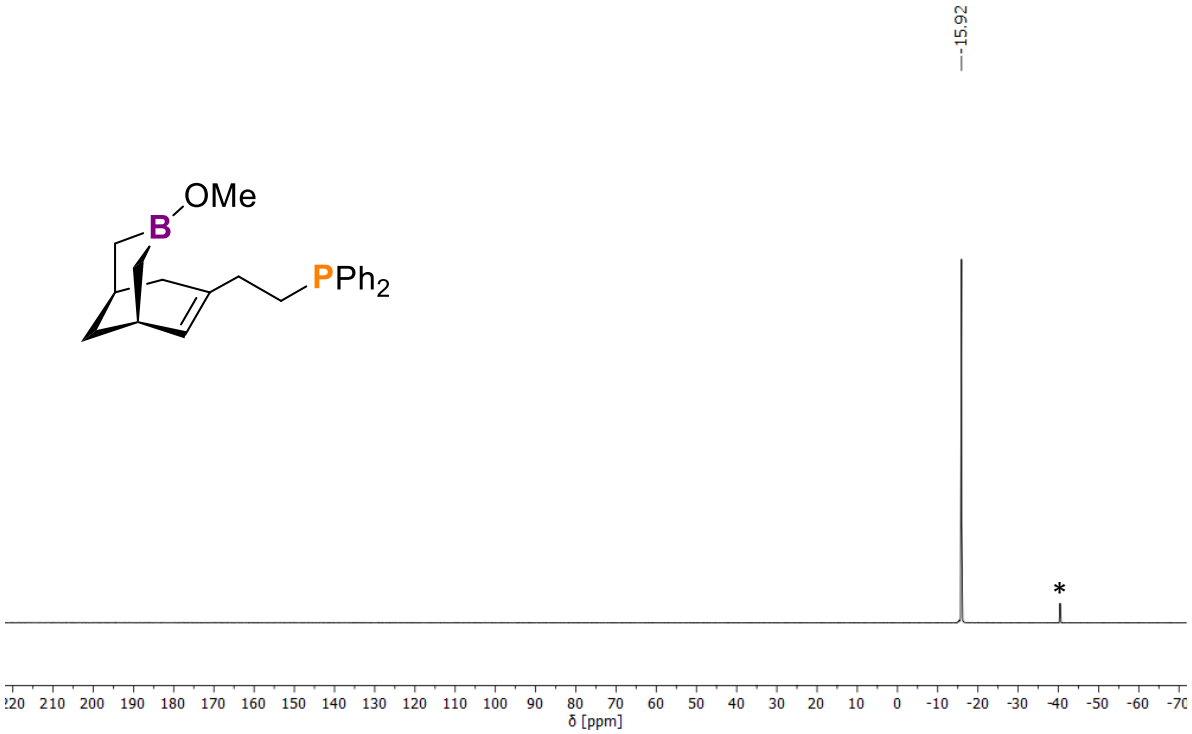

Figure S19: 6^{Ph}, $^{11}B\{^{1}H\}$ NMR, d$_1$-CDCl$_3$. 193 MHz, 298 K.

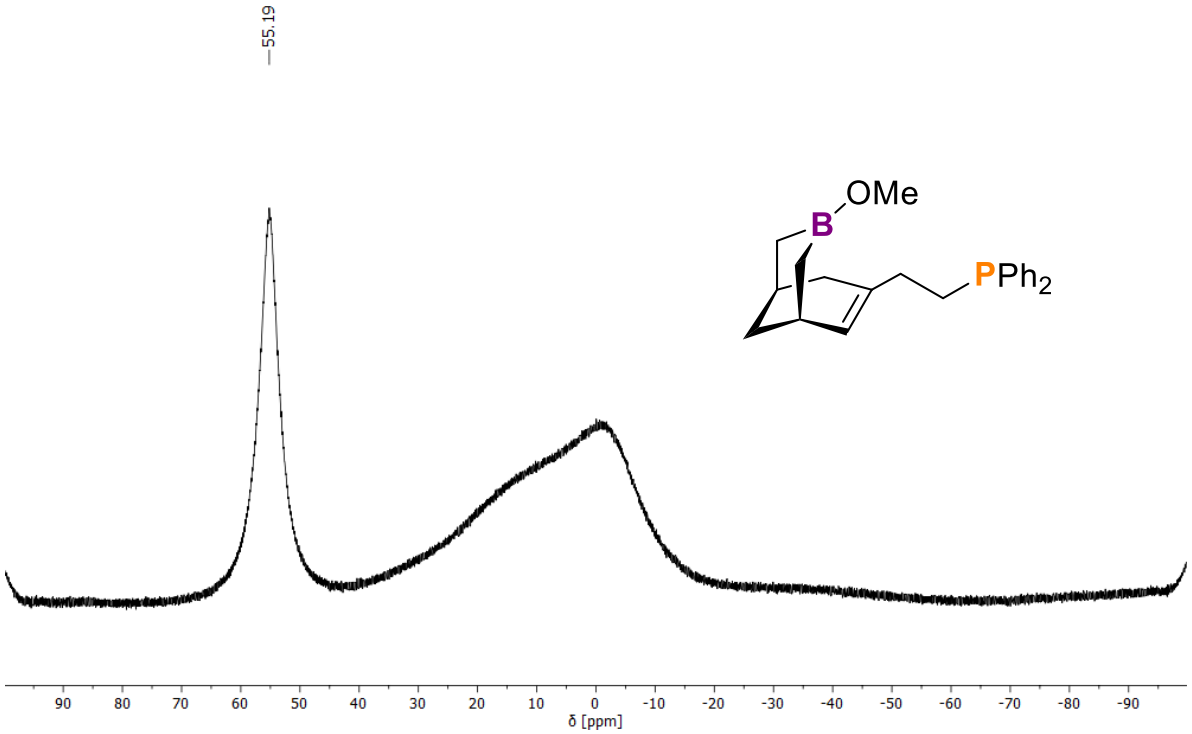

Figure S20: 6^{Ph}, $^{13}C\{^{1}H\}$ NMR, d$_1$-CDCl$_3$, 101 MHz, 298 K. * denotes residual *n*-pentane.

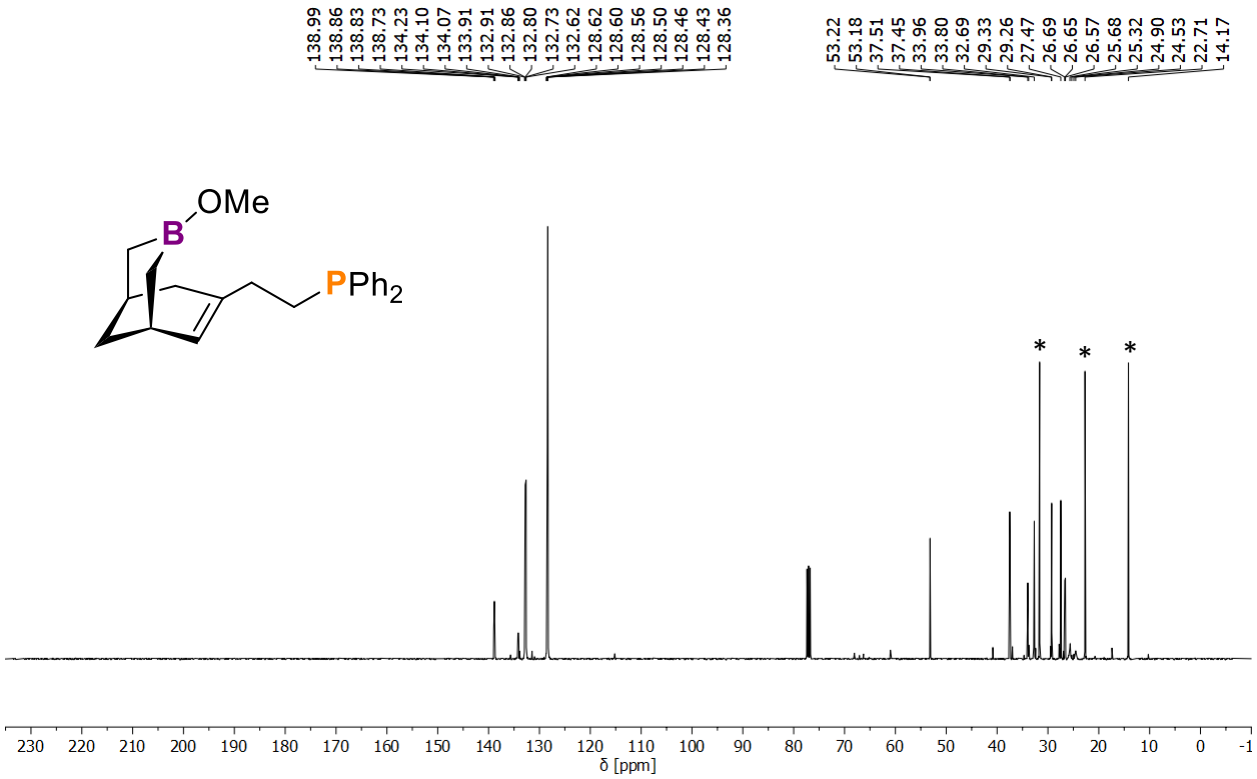

Figure S21: 7^{Ph}, ^{1}H NMR, d_8-THF, 600 MHz, 298 K. * denotes traces of silicon grease.

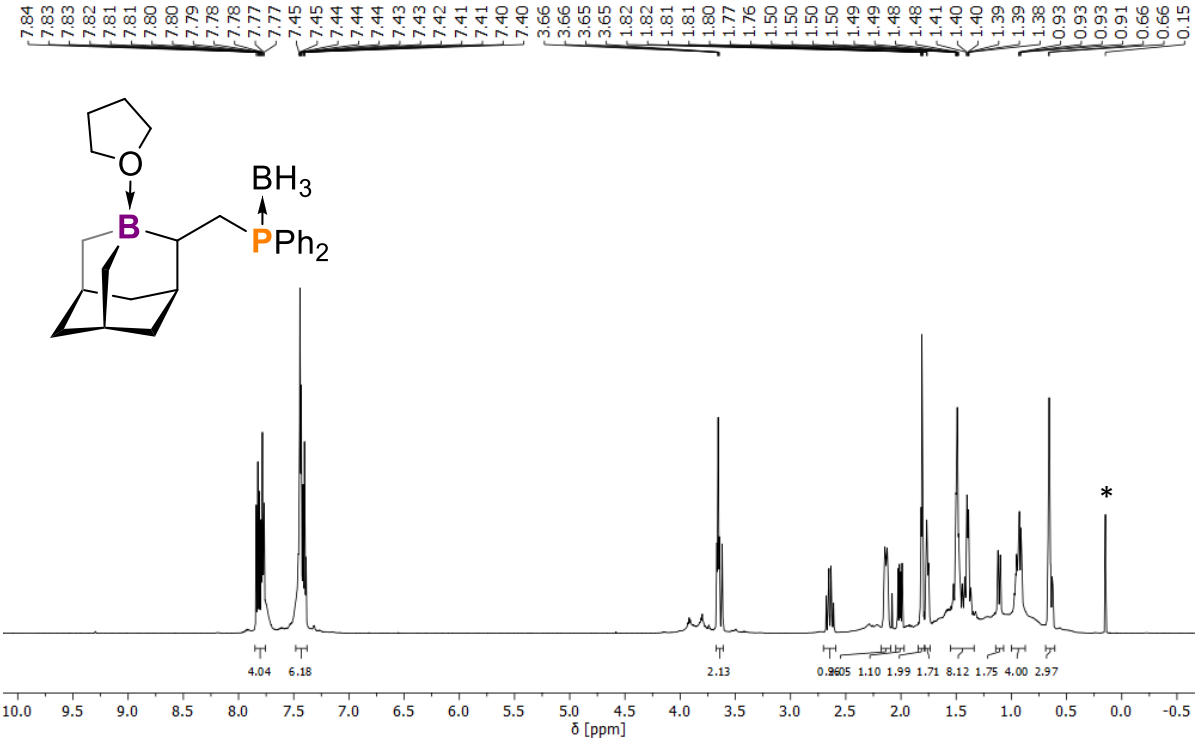

Figure S22: 7^{Ph}, $^{31}P\{^{1}H\}$ NMR, d_8-THF, 243 MHz, 298 K.

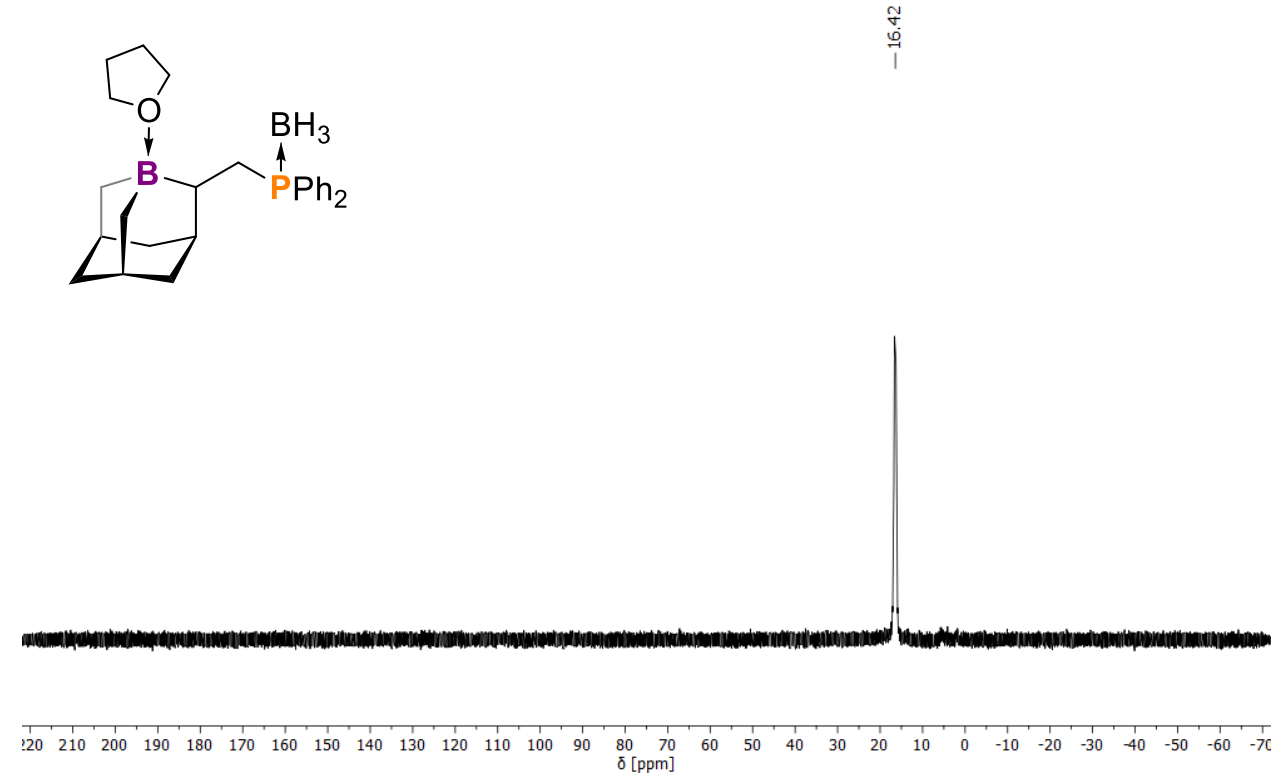

Figure S23: 7^{Ph}, $^{11}B\{^1H\}$ NMR, d_8-THF. 193 MHz, 298 K.

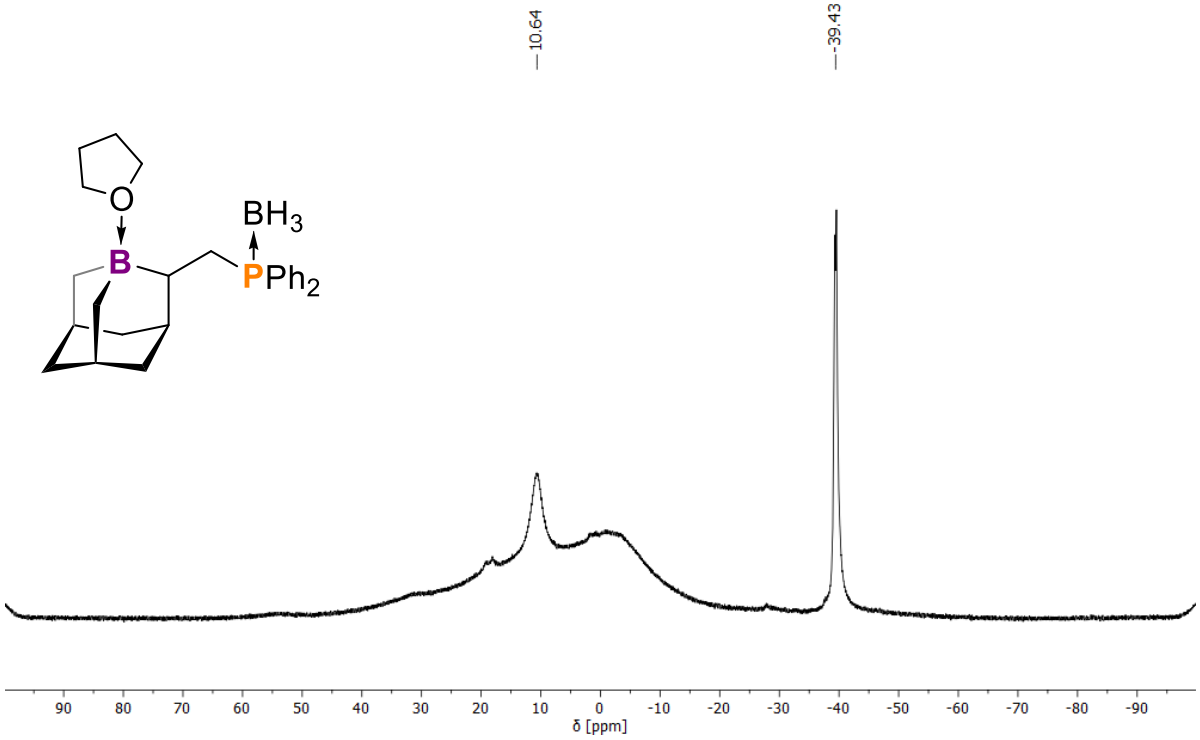

Figure S24: 7^{Ph}, $^{13}C\{^1H\}$ NMR, d_8-THF, 101 MHz, 298 K.

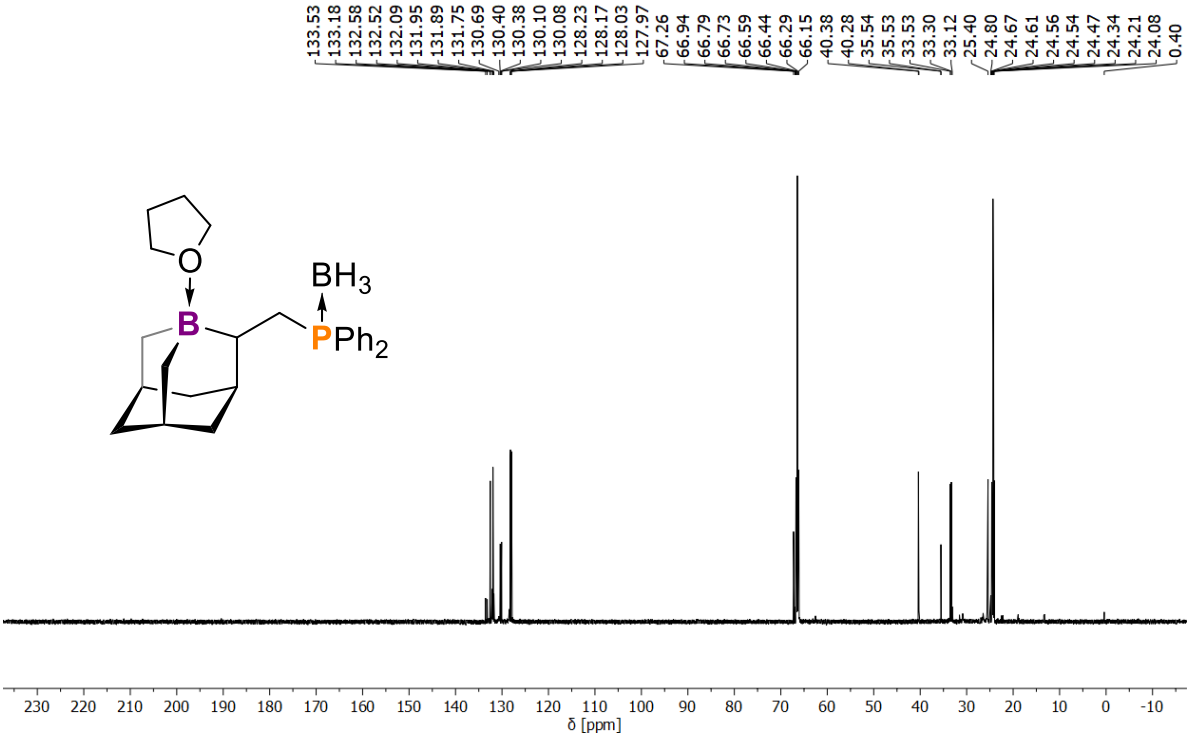

Figure S25: 8$^{t\text{-Bu}}$-DMAP, ^{1}H NMR, d$_6$-C$_6$D$_6$, 600 MHz, 298 K.

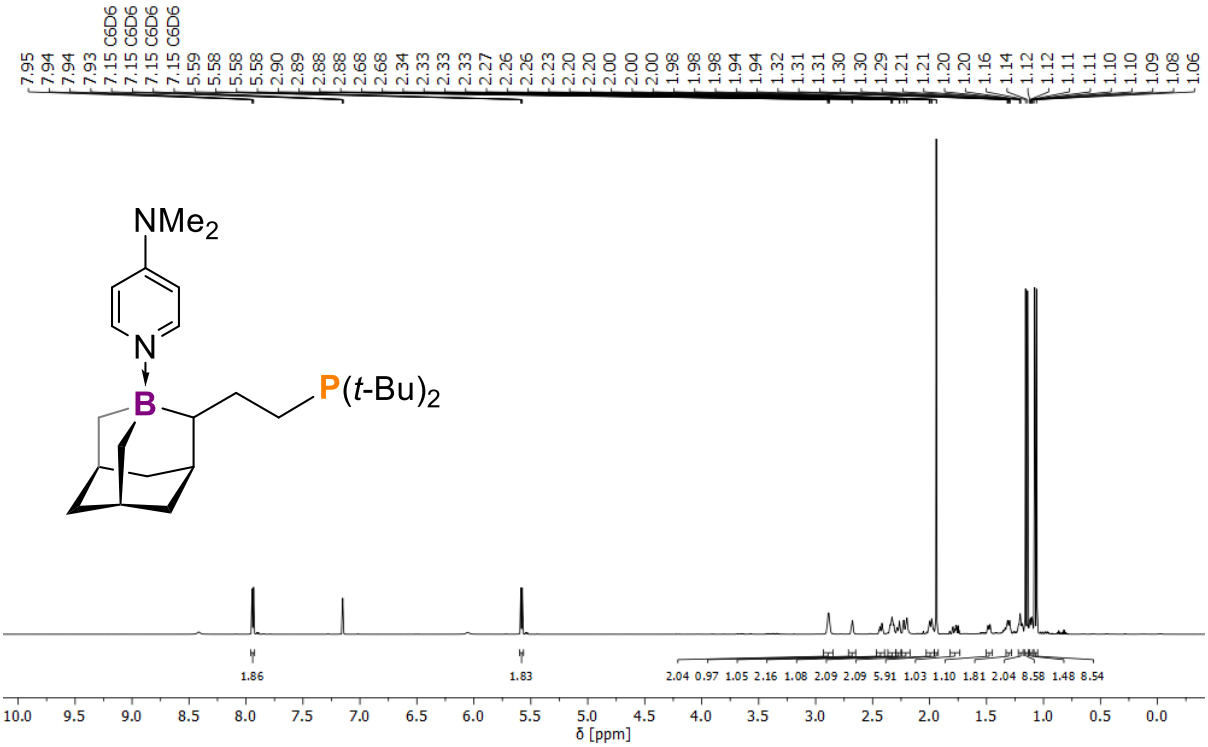

Figure S26: 8$^{t\text{-Bu}}$-DMAP, ^{31}P{^{1}H} NMR, d$_6$-C$_6$D$_6$, 243 MHz, 298 K.

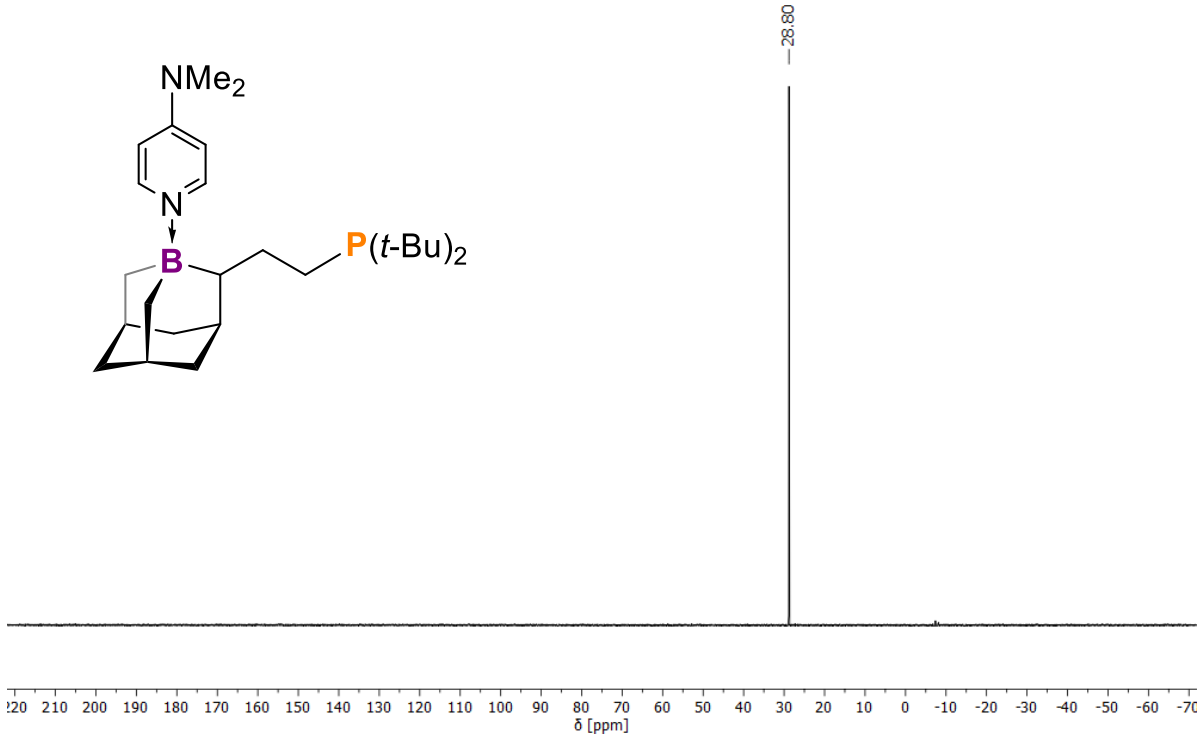

Figure S27: 8$^{t\text{-Bu}}$-DMAP, $^{11}B\{^{1}H\}$ NMR, d$_6$-C$_6$D$_6$. 193 MHz, 298 K.

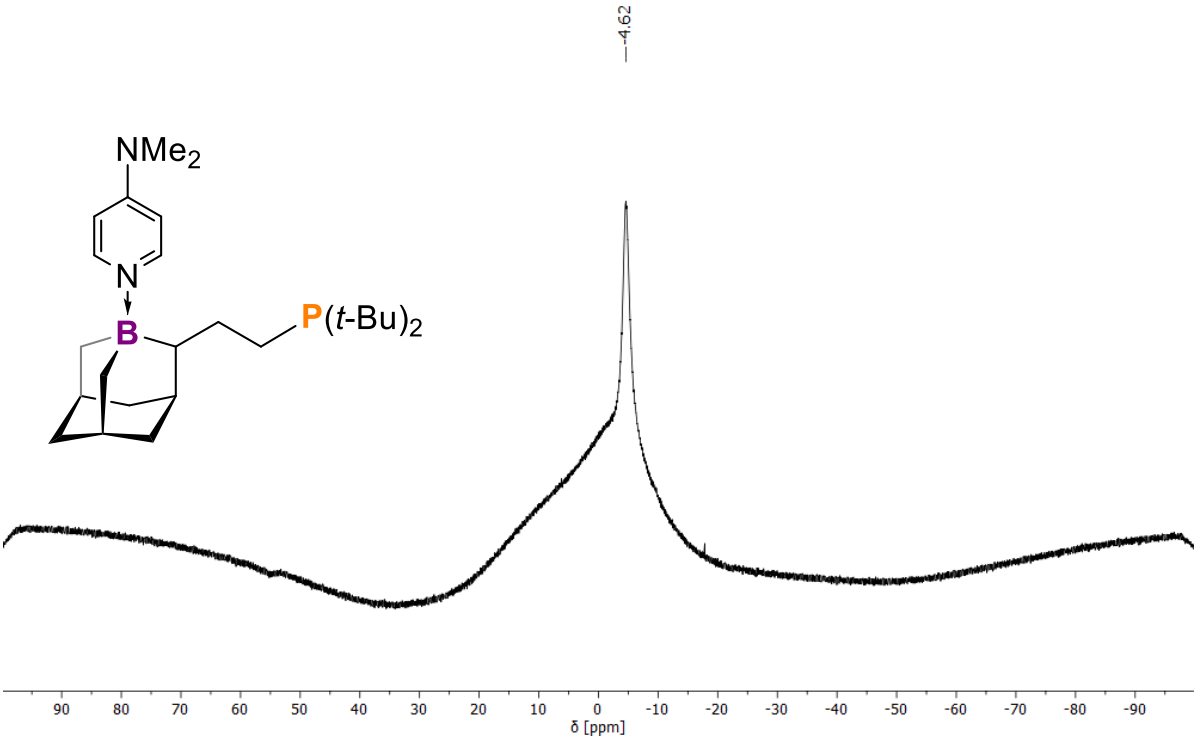

Figure S28: 8$^{t\text{-Bu}}$-DMAP, $^{13}C\{^{1}H\}$ NMR, d$_6$-C$_6$D$_6$, 101 MHz, 298 K.

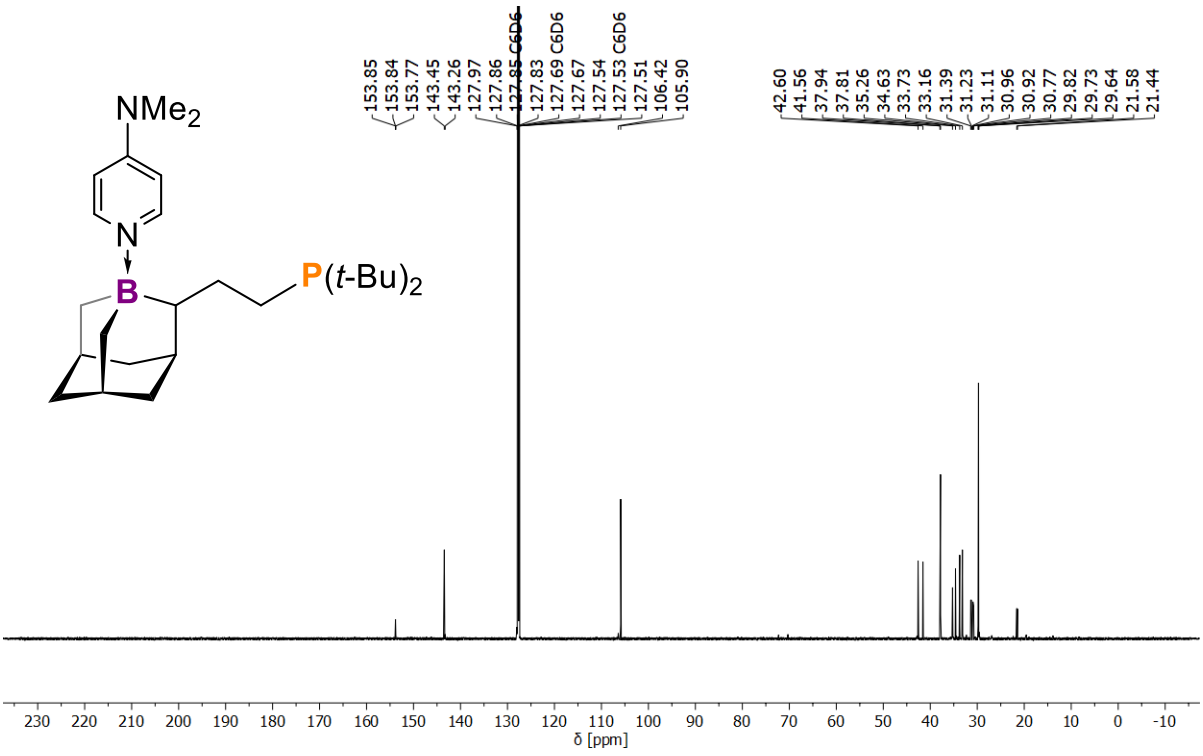

Figure S29: 8$^{t\text{-Bu}}$-HNEt$_2$, ^{1}H NMR, d$_6$-C$_6$D$_6$, 600 MHz, 298 K.

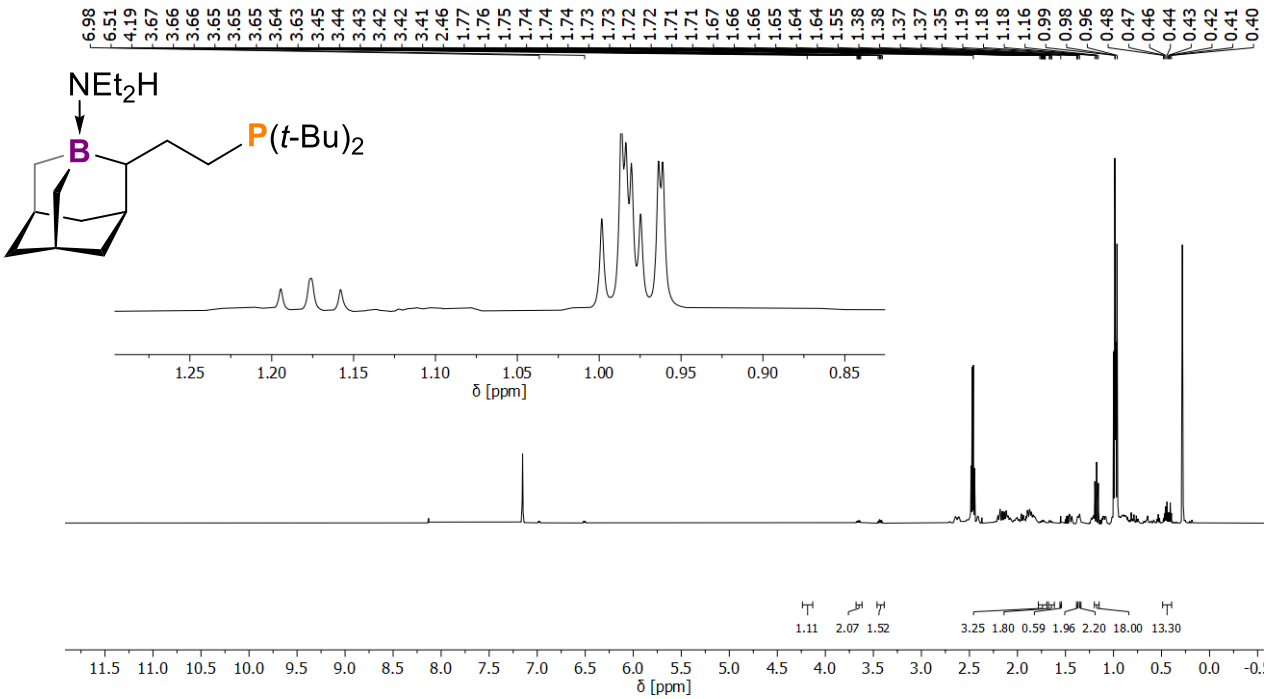

Figure S30: 8$^{t\text{-Bu}}$-HNEt$_2$, ^{31}P{^{1}H} NMR, d$_6$-C$_6$D$_6$, 243 MHz, 298 K. Top: equimolar amounts **4$^{t\text{-Bu}}$:** HNEt$_2$; Middle: 26 eq. HNEt$_2$; Bottom: remaining material after all volatiles have been removed.

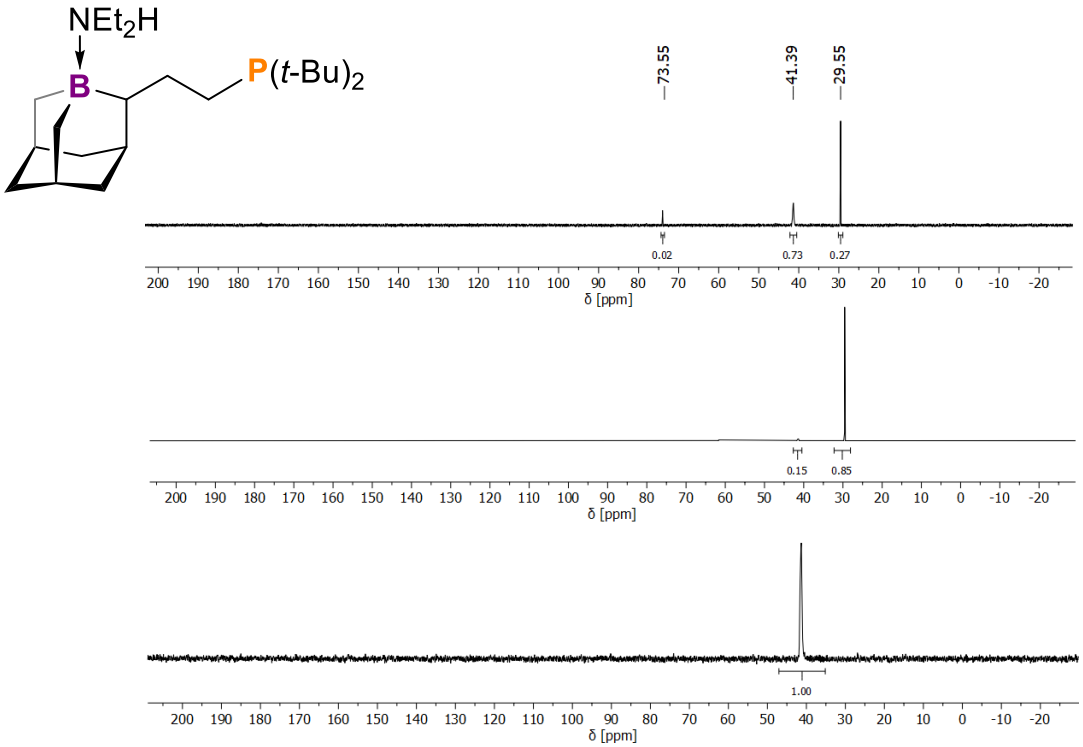

Figure S31: 8$^{t\text{-Bu}}$-HNEt$_2$, ^{11}B{^{1}H} NMR, d$_6$-C$_6$D$_6$. 193 MHz, 298 K.

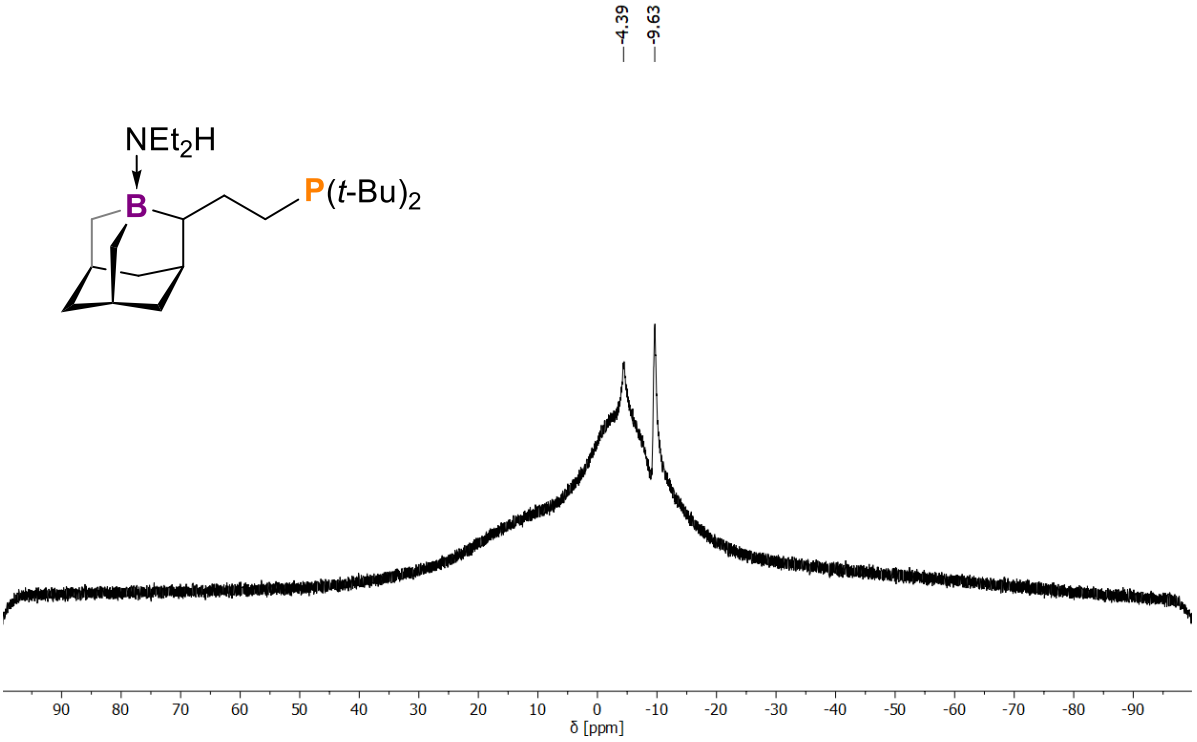

Figure S32: 9$^{t\text{-Bu}}$, ^{1}H NMR, d$_6$-C$_6$D$_6$, 600 MHz, 298 K.

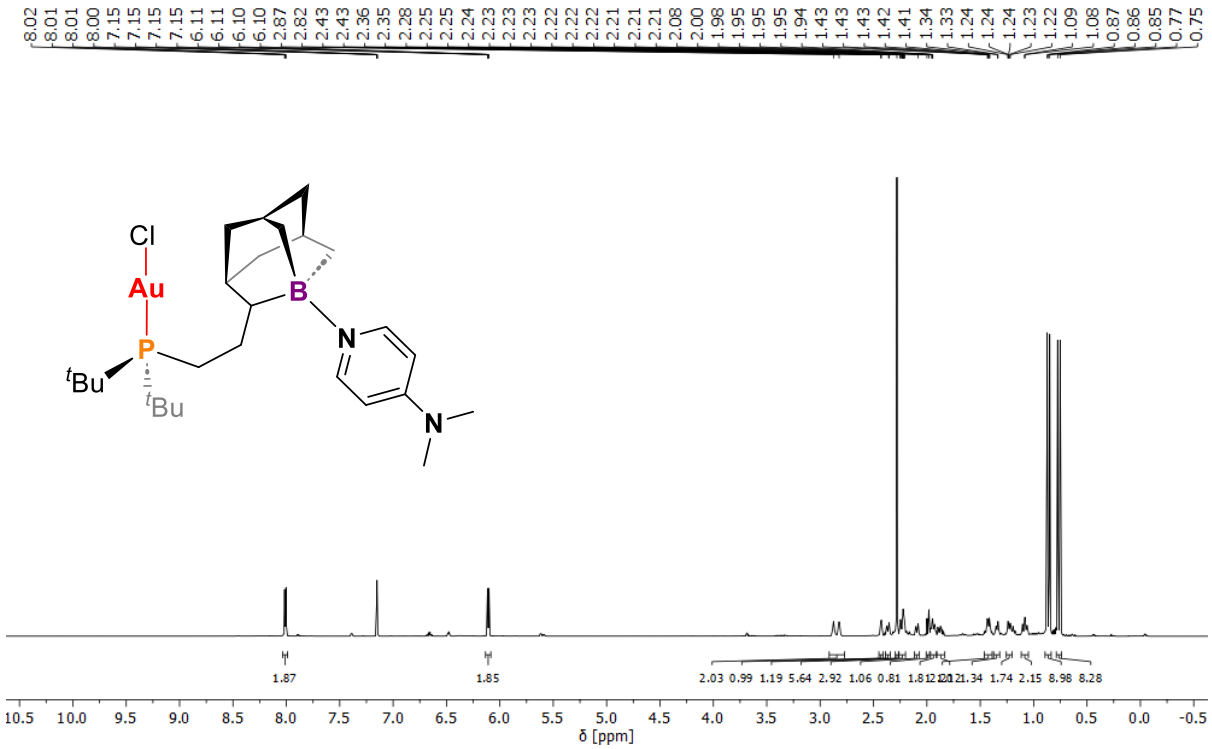

Figure S33: 9$^{t\text{-Bu}}$, $^{31}P\{^{1}H\}$ NMR, d$_6$-C$_6$D$_6$, 243 MHz, 298 K. $^{11}B\{^{1}H\}$ NMR, d$_6$-C$_6$D$_6$. 193 MHz, 298 K. * denotes unknown impurity.

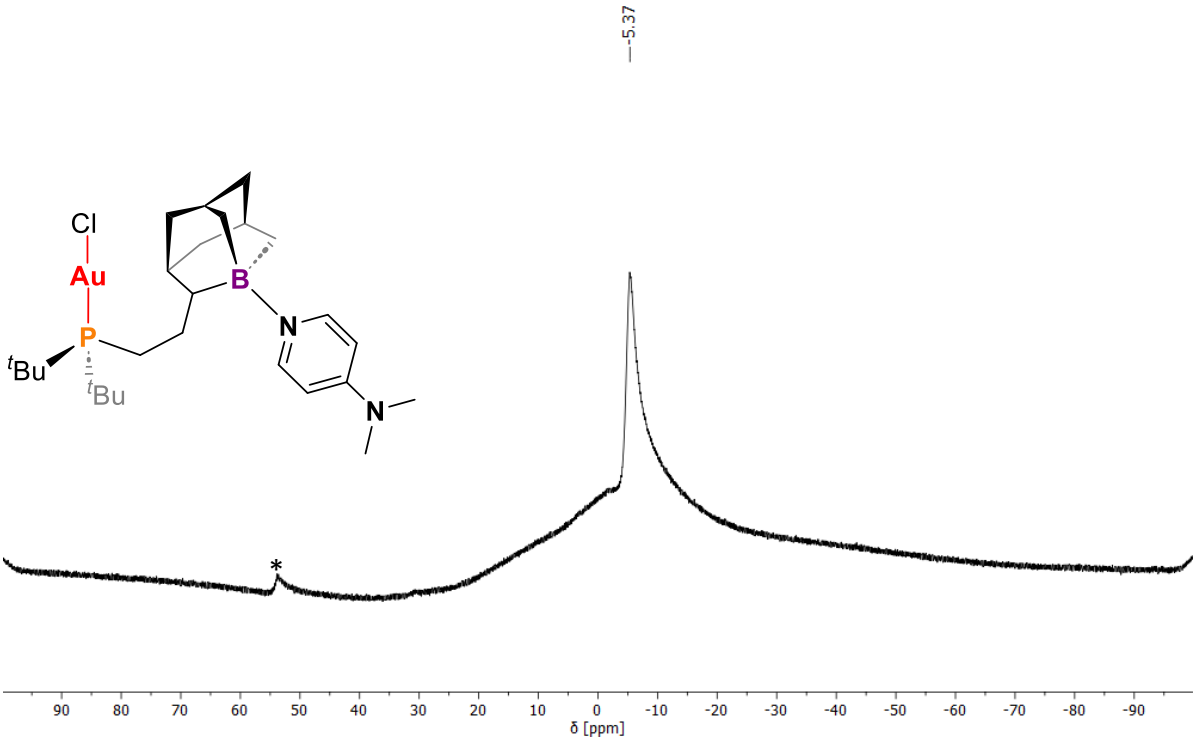

Figure S34: 9$^{t\text{-Bu}}$, 9$^{t\text{-Bu}}$, $^{31}P\{^{1}H\}$ NMR, d$_6$-C$_6$D$_6$, 243 MHz, 298 K.

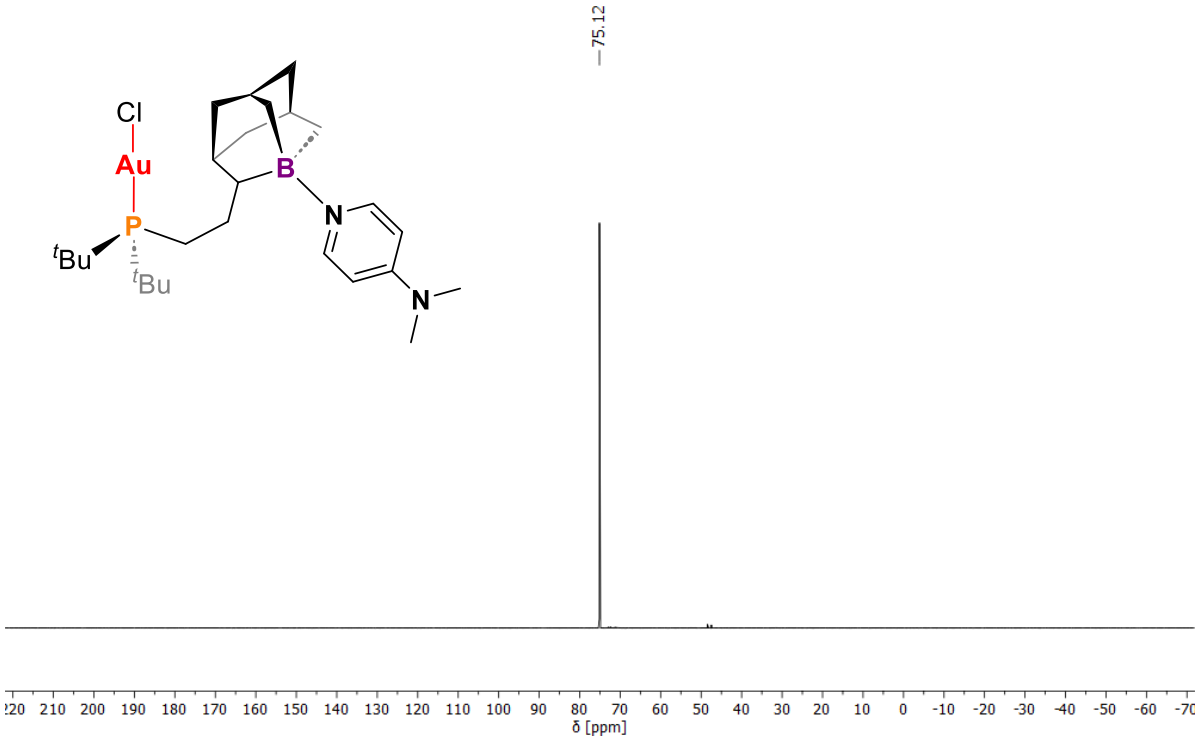

Figure S35: 9$^{t\text{-Bu}}$, $^{13}C\{^{1}H\}$ NMR, d6-C_6D_6, 101 MHz, 298 K.

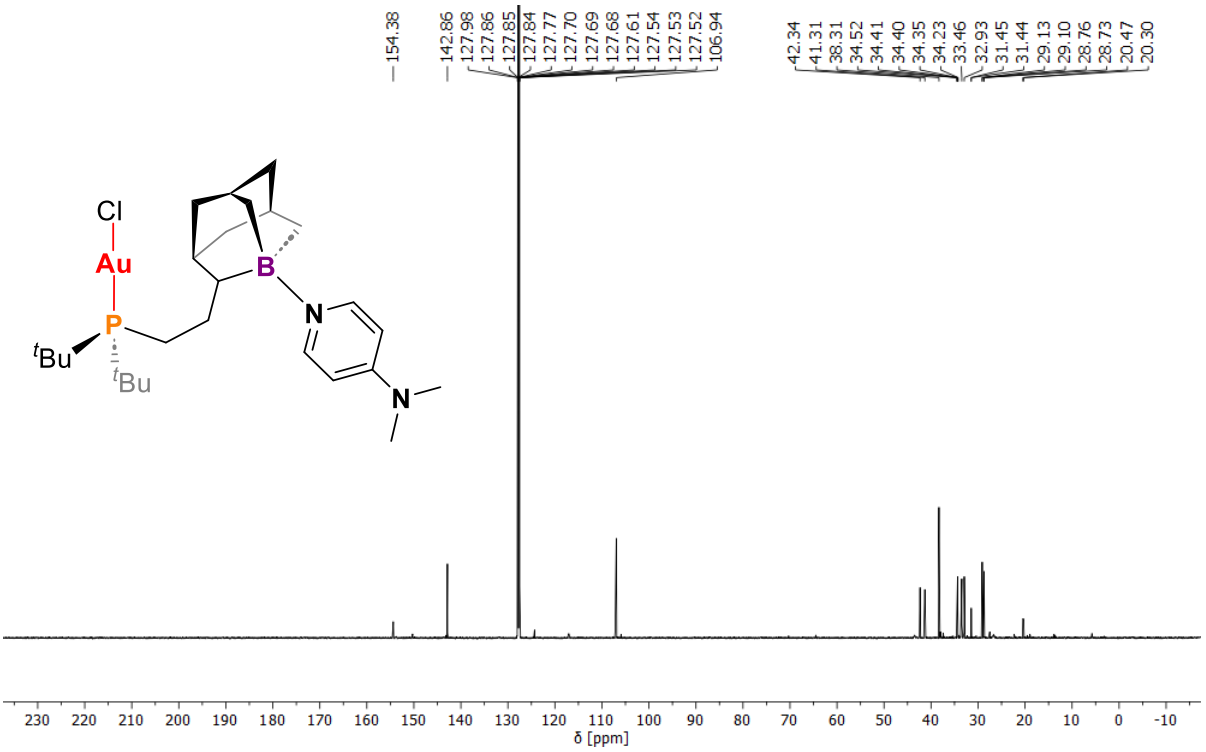

Figure S36: 10$^{t\text{-Bu}}$, ^{1}H NMR, d8-THF, 600 MHz, 298 K.

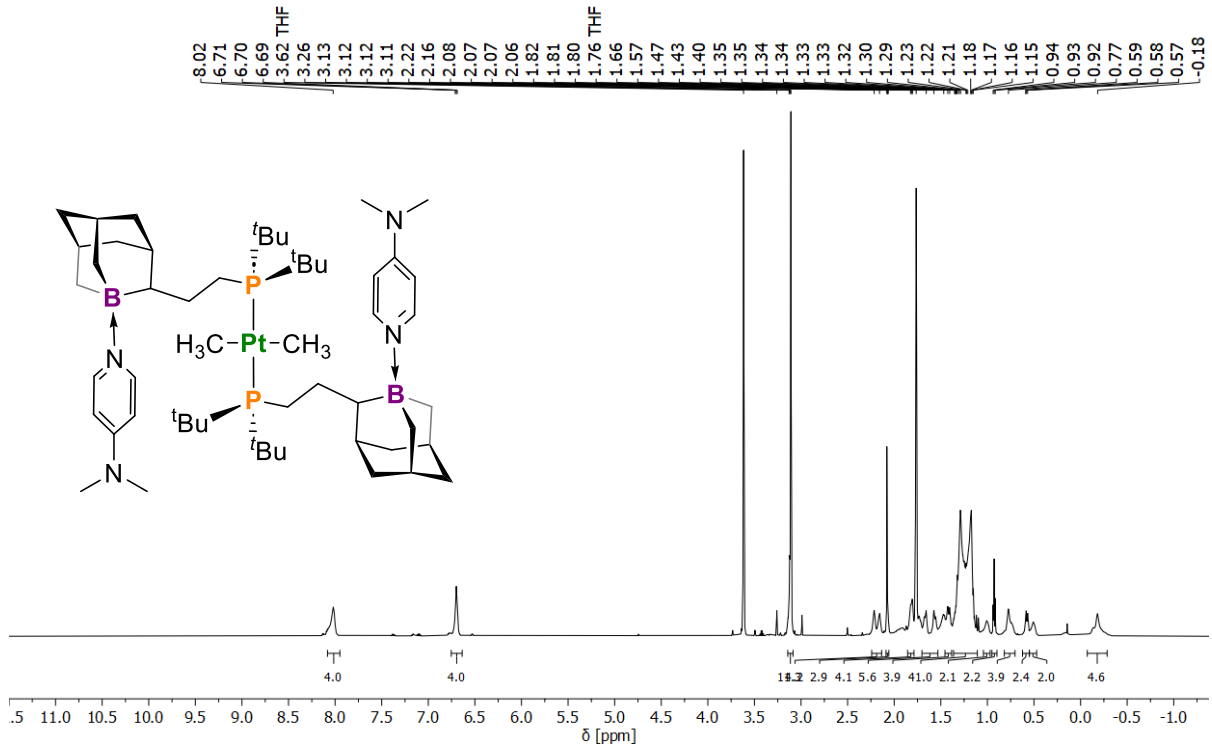

Figure S37: 10$^{t\text{-Bu}}$, $^{11}B\{^{1}H\}$ NMR, d_8-THF. 193 MHz, 298 K.

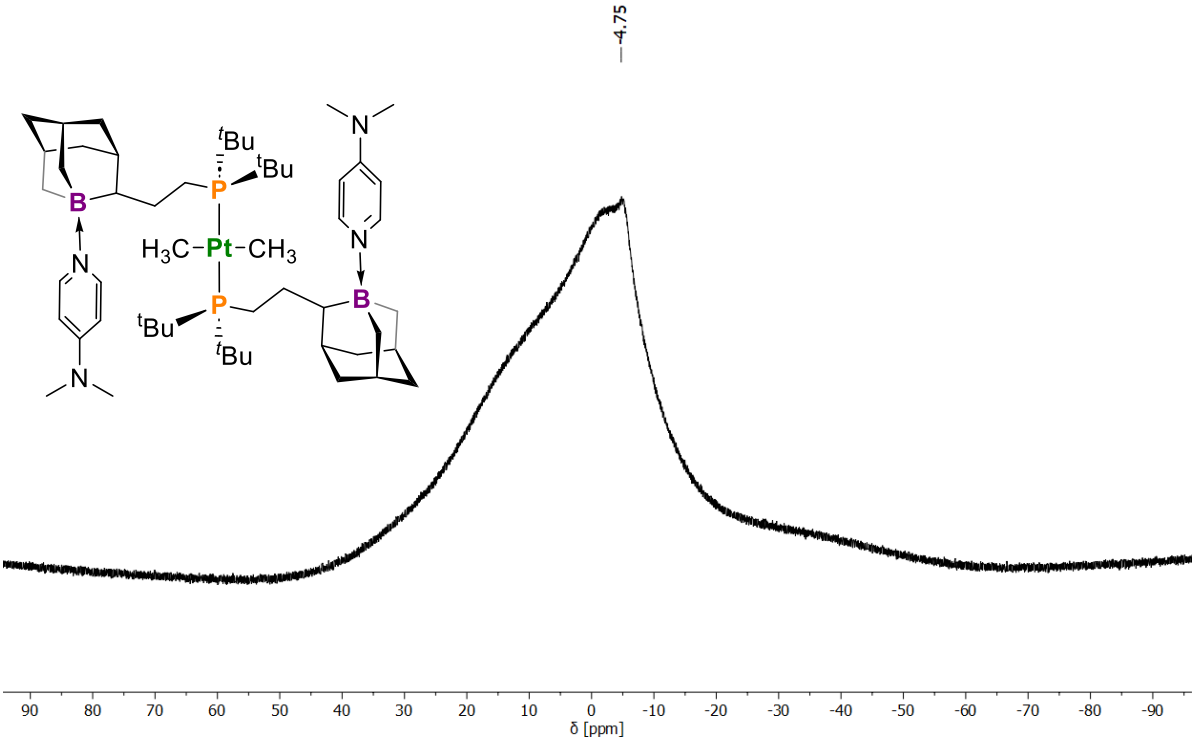

Figure S38: 10$^{t\text{-Bu}}$, $^{31}P\{^{1}H\}$ NMR, d_8-THF, 243 MHz, 298 K.

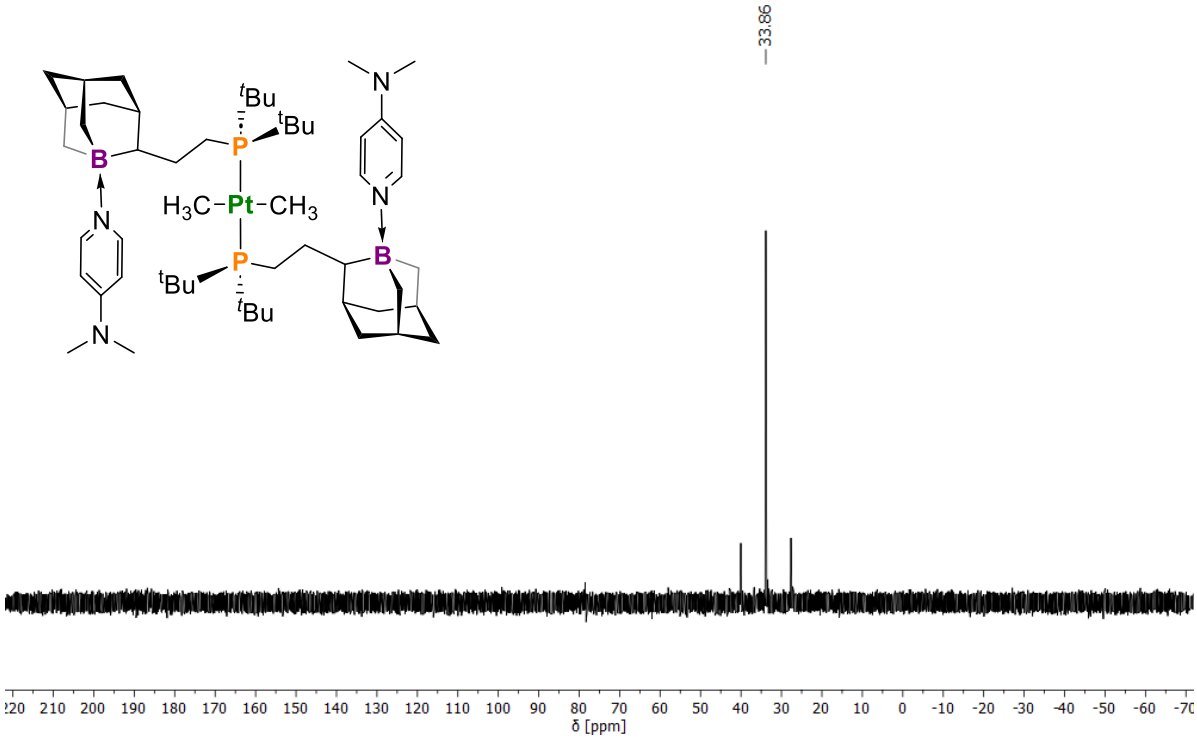

Figure S39: 10$^{t\text{-Bu}}$, $^{13}C\{^{1}H\}$ NMR, d$_8$-THF, 101 MHz, 298 K.

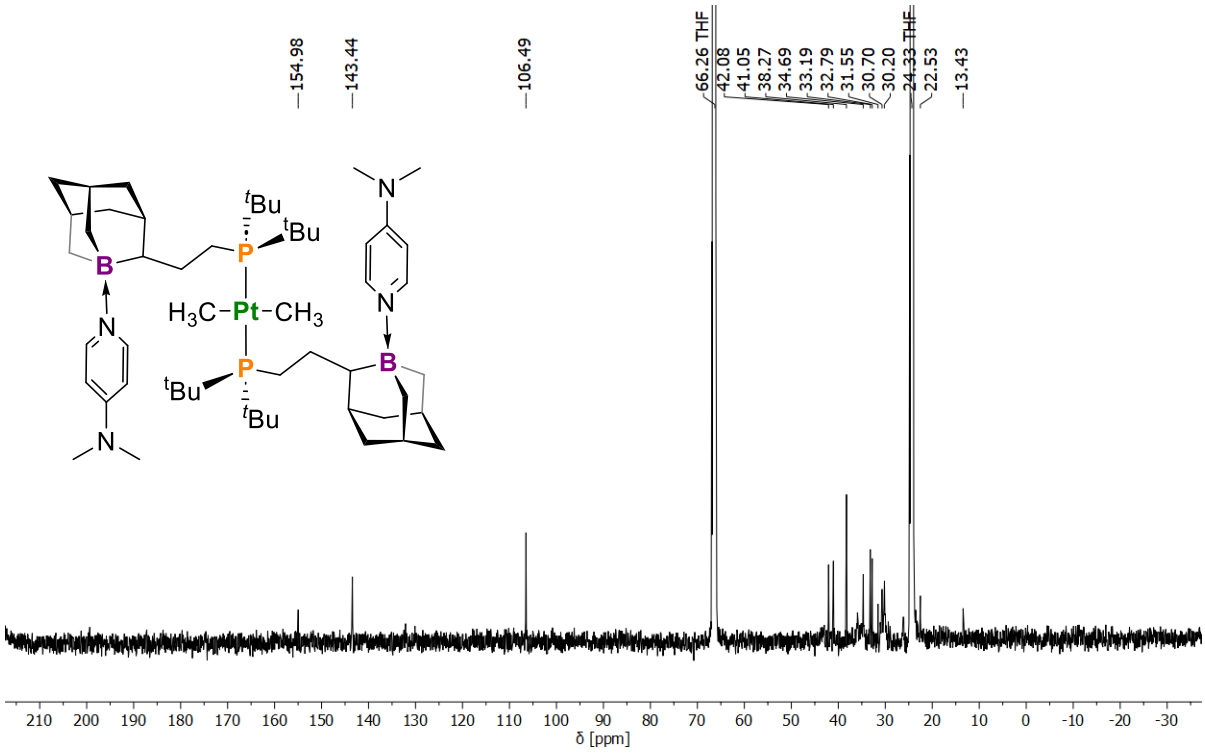

Additional reactions:

i. Reaction of $4^{t\text{-Bu}}$ with CO_2 and H_2.

In a typical experiment, $\mathbf{4}^{t\text{-Bu}}$ (30 mg, 0.098 mmol) was dissolved in 20 mL *n*-pentane and placed in a Schlenk bomb. The solution was degassed with three freeze-pump-thaw cycles and subsequently an atmosphere of CO_2 or H_2 was added. After stirring overnight, an aliquot was analyzed by $^{31}P\{^1H\}$ NMR spectroscopy indicating no reaction (**Figures S40** and **S41**).

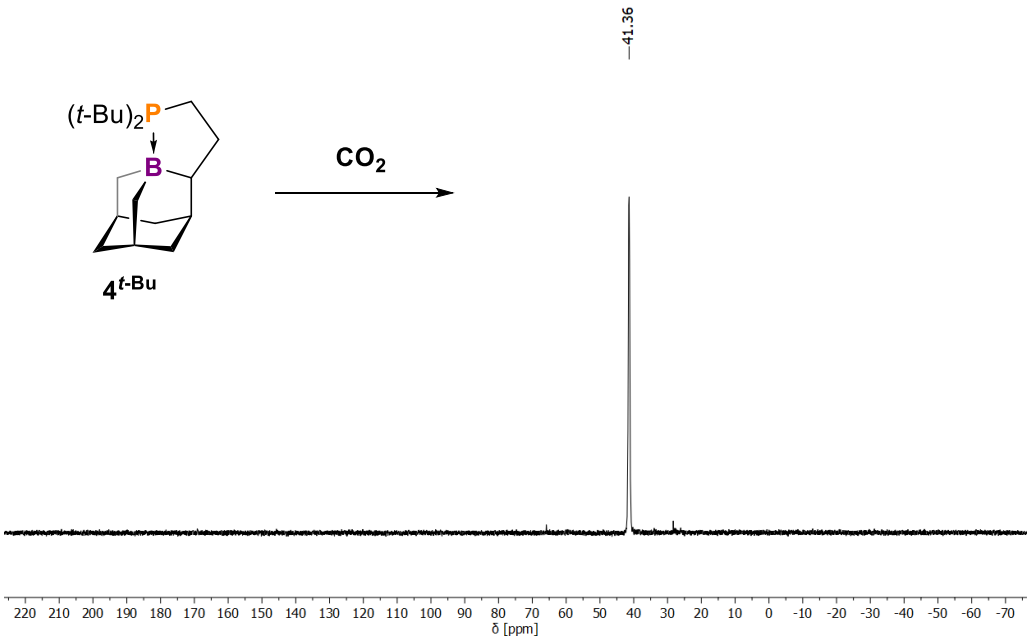

Figure S40: Reaction of $4^{t\text{-Bu}}$ with CO_2, $^{31}P\{^1H\}$ NMR, d_6-C_6D_6, 243 MHz, 298 K.

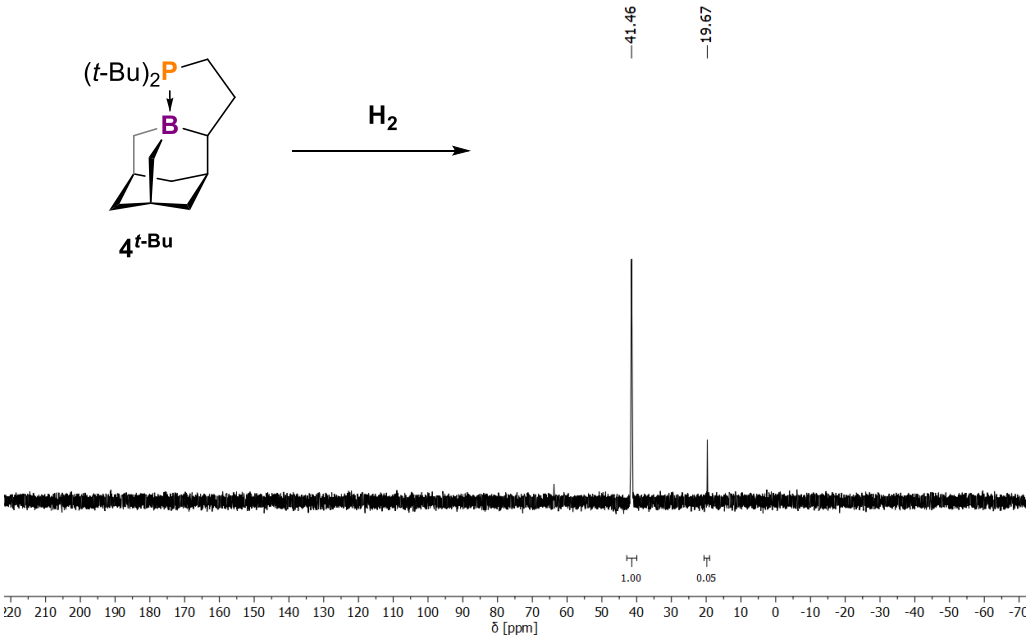

Figure S41: Reaction of $4^{t\text{-Bu}}$ with H_2, $^{31}P\{^1H\}$ NMR, d_6-C_6D_6, 243 MHz, 298 K.

ii. Reaction of $4^{t\text{-Bu}}$ with Lewis Bases.

Additional Lewis bases of different donor strength were added to $\mathbf{4}^{t\text{-Bu}}$ to investigate potential for P-B ring-opening.

Reaction:

1) $\mathbf{4}^{t\text{-Bu}}$ + pyridine → ring opening

10 mg of $\mathbf{4}^{t\text{-Bu}}$ was weighed into a 20 mL scintillation vial and dissolved in 500 µL C_6D_6. 1 equivalent of pyridine was added. Ring-opening was concluded by $^{31}P\{^1H\}$ NMR spectroscopy (**Figure S42**).

2) $\mathbf{4}^{t\text{-Bu}}$ + DMSO → no reaction

10 mg of $\mathbf{4}^{t\text{-Bu}}$ was weighed into a 20 mL scintillation vial and dissolved in 500 µL C_6D_6. 1 equivalent of DMSO-d_6 was added. No reaction was observed by $^{31}P\{^1H\}$ NMR spectroscopy (**Figure S43**).

3) $\mathbf{4}^{t\text{-Bu}}$ + DMF → no reaction

10 mg of $\mathbf{4}^{t\text{-Bu}}$ was weighed into a 20 mL scintillation vial and dissolved in 500 µL C_6D_6. 1 equivalent of DMF was added. No reaction was observed by $^{31}P\{^1H\}$ NMR spectroscopy (**Figure S44**).

4) $\mathbf{4}^{t\text{-Bu}}$ + NEt_3 → no reaction

10 mg of $\mathbf{4}^{t\text{-Bu}}$ was weighed into a 20 mL scintillation vial and dissolved in 500 µL C_6D_6. 1 equivalent of $NEt_3$was added. No reaction was observed by $^{31}P\{^1H\}$ NMR spectroscopy (**Figure S45**).

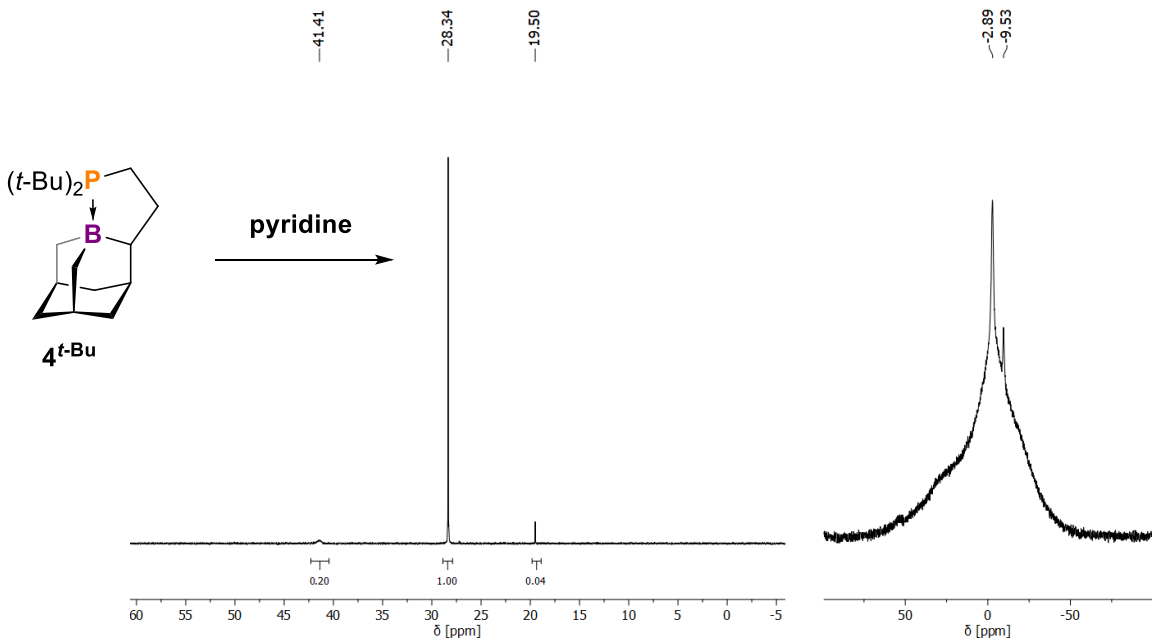

Figure S42: Reaction of $4^{t\text{-Bu}}$ with pyridine, left: $^{31}P\{^{1}H\}$ NMR, d6-C6D6, 243 MHz, 298 K; right: $^{11}B\{^{1}H\}$ NMR, d6-C6D6, 193 MHz, 298 K.

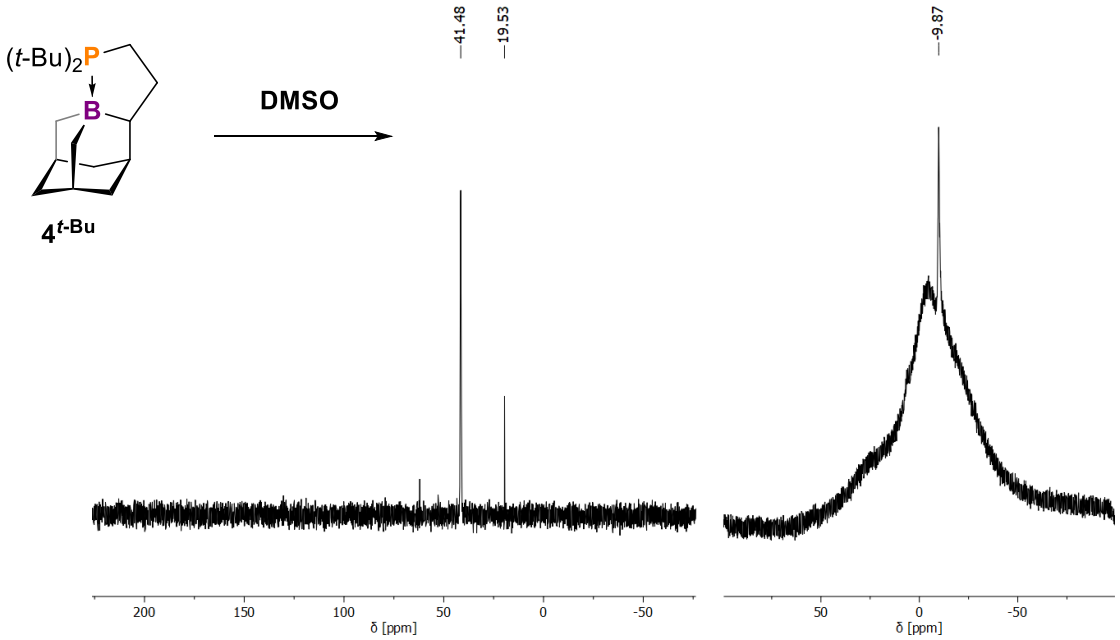

Figure S43: Reaction of $4^{t\text{-Bu}}$ with DMSO, left: $^{31}P\{^{1}H\}$ NMR, d6-C6D6, 243 MHz, 298 K; right: $^{11}B\{^{1}H\}$ NMR, d6-C6D6, 193 MHz, 298 K.

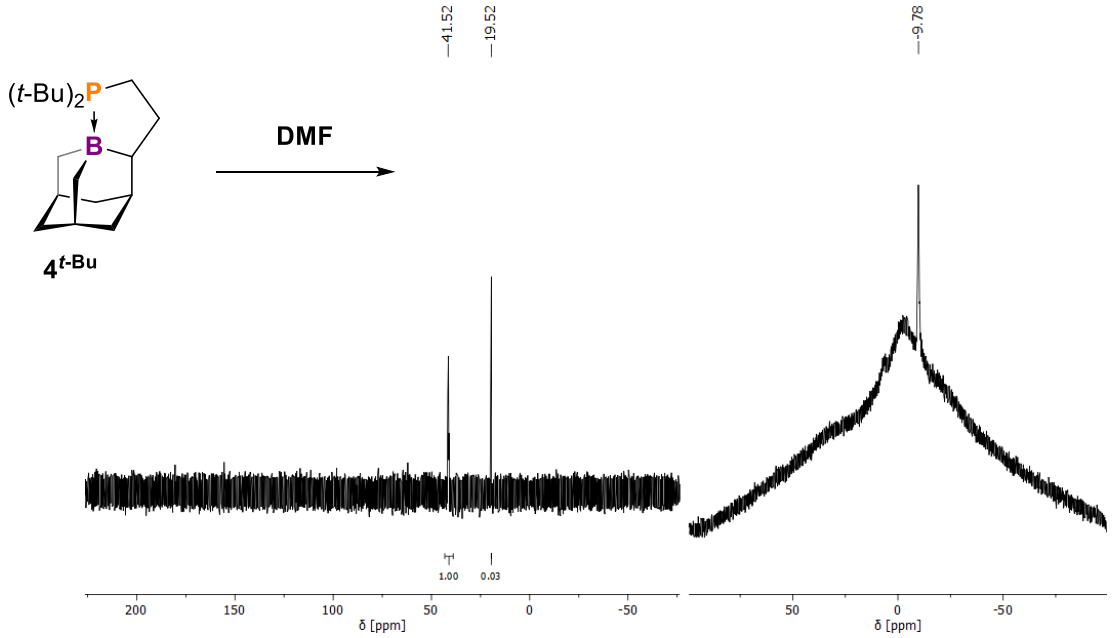

Figure S44: Reaction of $4^{t\text{-Bu}}$ with DMF, left: $^{31}P\{^{1}H\}$ NMR, d6-C6D6, 243 MHz, 298 K; right: $^{11}B\{^{1}H\}$ NMR, d6-C6D6, 193 MHz, 298 K.

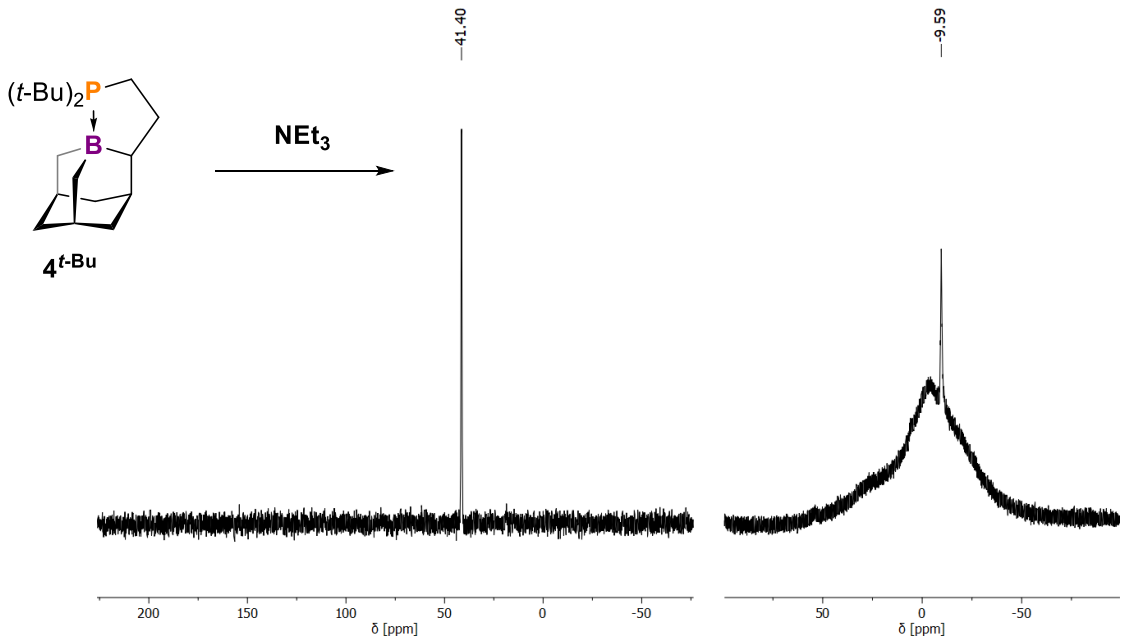

Figure S45: Reaction of $4^{t\text{-Bu}}$ with NEt_3, left: $^{31}P\{^{1}H\}$ NMR, d6-C6D6, 243 MHz, 298 K; right: $^{11}B\{^{1}H\}$ NMR, d6-C6D6, 193 MHz, 298 K.

iii. Reaction of $\mathbf{4}^{t\text{-Bu}}$ with Lewis Acids or a Hydride Source.

Ring-opening reactions were attempted by treating $\mathbf{4}^{t\text{-Bu}}$ with acids: $[H(Et_2O)_2]B(C_6F_5)_4$, $[AuCl(SMe_2)]$, or a hydride source, $Li[HBEt_3]$.

Reaction:

1) $\mathbf{4}^{t\text{-Bu}}$ + $[H(Et_2O)_2]B(C_6F_5)_4$ → ring-opening

10 mg of $\mathbf{4}^{t\text{-Bu}}$ was weighed into a 20 mL scintillation vial and dissolved in 500 μL fluorobenzene. 1 equivalent of $[H(Et_2O)_2]B(C_6F_5)_4$ was added. Volatiles were removed *in vacuo* and the sample was redissolved in THF-d_8. A main phosphonium species along with several side products was observed (**Figures S46** and **S47**).

2) $\mathbf{4}^{t\text{-Bu}}$ + $[AuCl(SMe_2)]$ → multiple products

21 mg of $\mathbf{4}^{t\text{-Bu}}$ was weighed into a 20 mL scintillation vial and dissolved in 2 mL of *ortho*-difluorobenzene (*o*-DFB). 1 equivalent of $[AuCl(SMe_2)]$ dissolved in 2 mL of *o*-DFB was added. The mixture was stirred for 2 h and filtered through celite. All volatiles were removed *in-vacuo* and the residual solid dissolved in C_6D_6 (**Figure S48**).

3) $\mathbf{4}^{t\text{-Bu}}$ + $LiHBEt_3$ → no reaction

$\mathbf{4}^{t\text{-Bu}}$ (10 mg, X mmol) was weighed into a 20 mL scintillation vial and dissolved in 500 μL THF. 1 equivalent of $LiBHEt_3$ was added. No reaction was observed by $^{31}P\{^1H\}$ NMR spectroscopy (**Figure S49**).

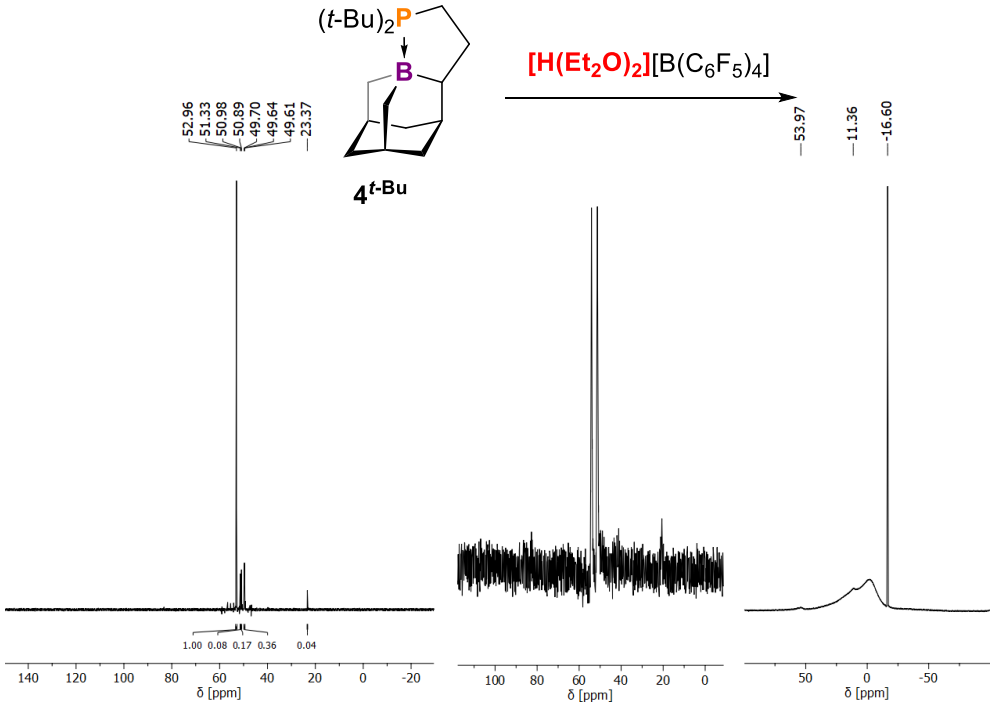

Figure S46: Reaction of $4^{t\text{-Bu}}$ with $[H(Et_2O)_2][B(C_6F_5)_4]$, left: $^{31}P\{^1H\}$ NMR, d8-THF, 243 MHz, 298 K; middle: ^{31}P NMR, d8-THF, 162 MHz, 298 K δ = 53 (d, J = 451 Hz, P-H); right: $^{11}B\{^1H\}$ NMR, d8-THF, 193 MHz, 298 K.

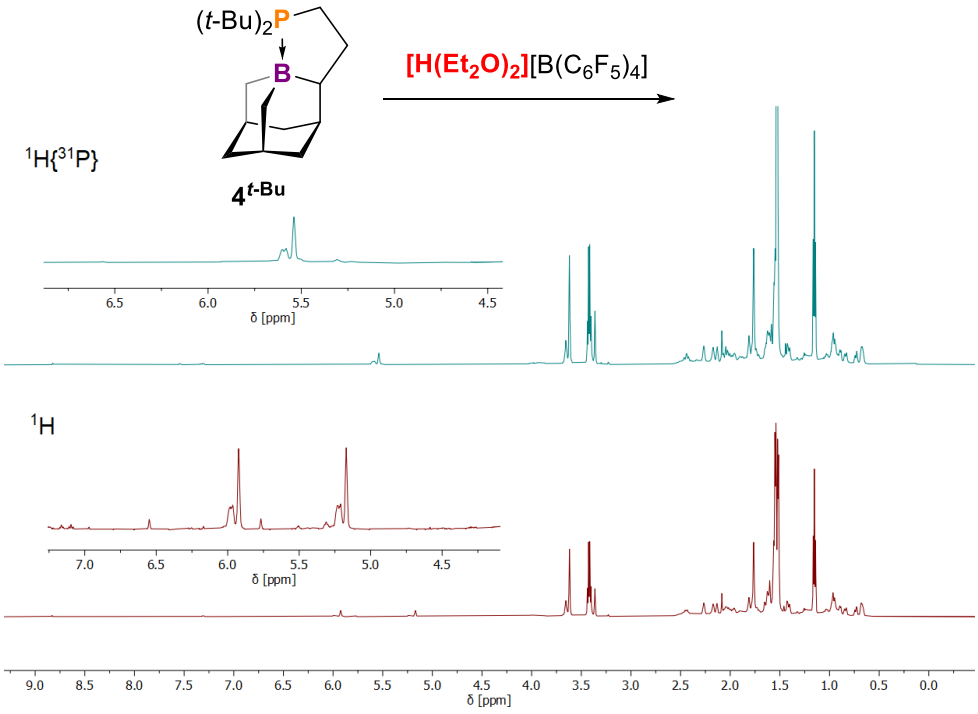

Figure S47: Reaction of $4^{t\text{-Bu}}$ with $[H(Et_2O)_2][B(C_6F_5)_4]$, top: $^1H\{^{31}P\}$ NMR, d8-THF, 243 MHz, 298 K; bottom: ^1H NMR, d8-THF, 193 MHz, 298 K. δ = 5.54 (d, J = 451 Hz, P-H)

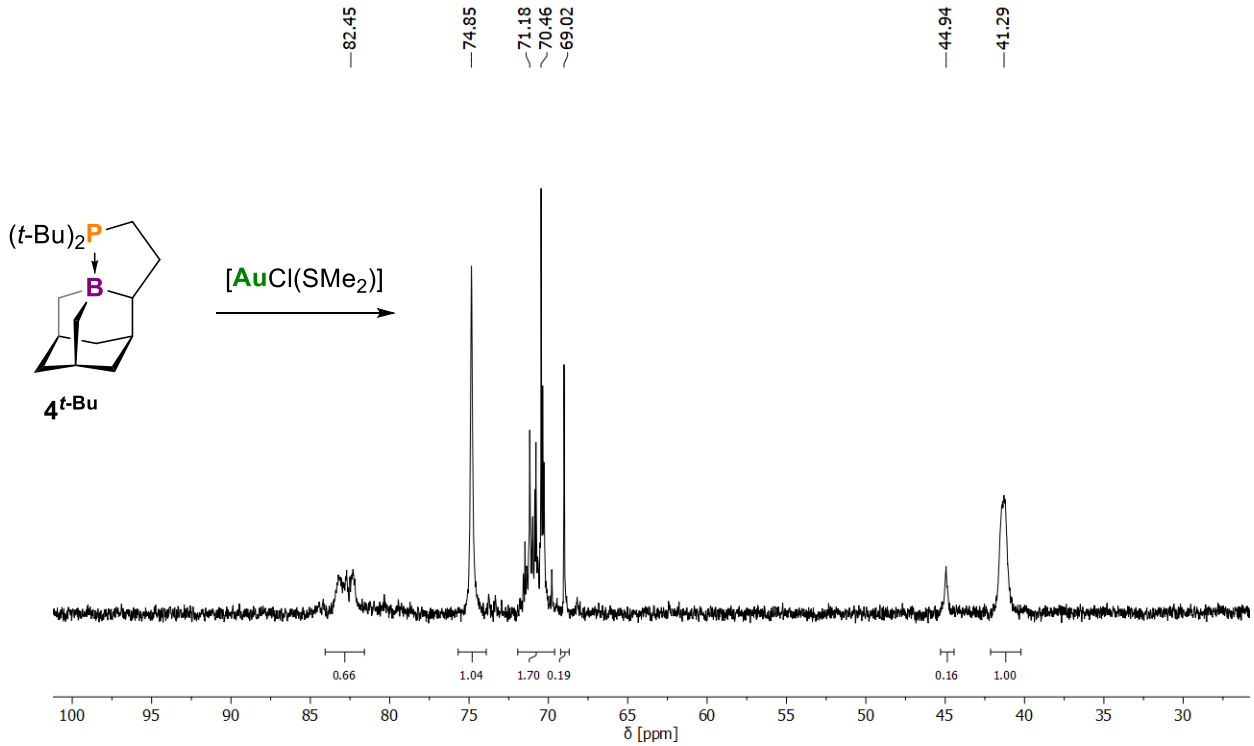

Figure S48: Reaction of $4^{t\text{-Bu}}$ with [AuCl(SMe$_2$)], $^{31}P\{^1H\}$ NMR, d_6-C_6D_6, 243 MHz, 298 K.

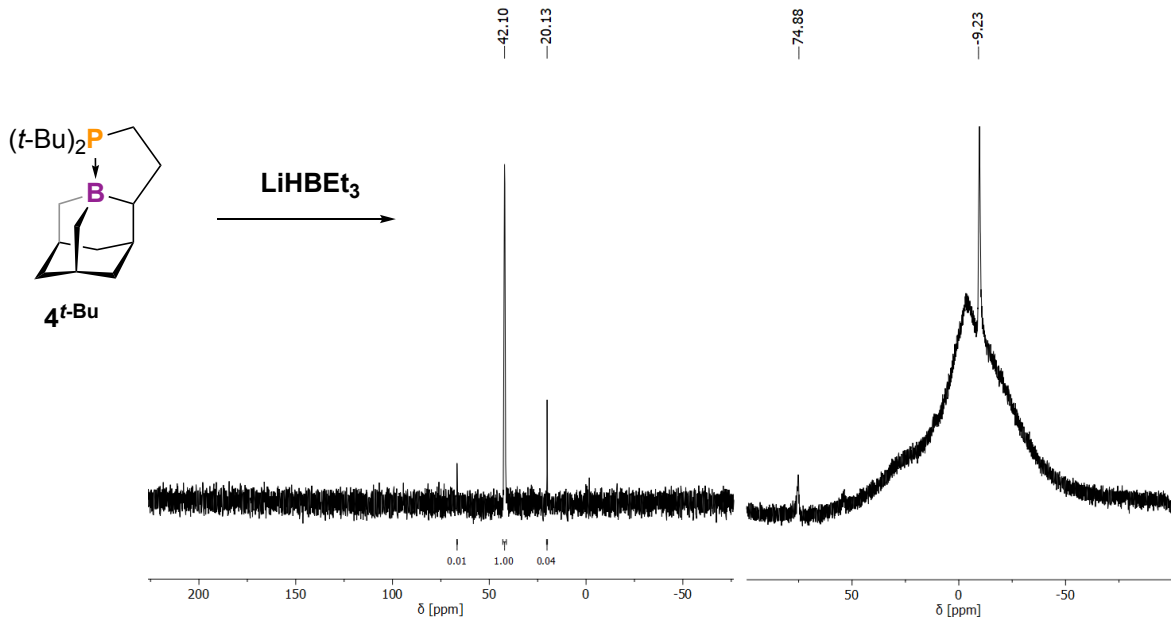

Figure S49: Reaction of $4^{t\text{-Bu}}$ with Li[HBEt$_3$], left: $^{31}P\{^1H\}$ NMR, THF, 243 MHz, 298 K; right: $^{11}B\{^1H\}$ NMR, THF, 193 MHz, 298 K.

iv. Attempts to deprotect 7^{Ph}

Reactions carried out to deprotect **7^{Ph}** (either at phosphorus or boron) included treatment with DABCO, $B(C_6F_5)_3$ (BCF), $[H(Et_2O)_2][B(C_6F_5)_4]$, NaO*t*Bu, and Verkade Base. These reactions were not clean and in the case of base addition, often yielded base-coordinated boraadamantanes.

Reaction:

7^{Ph} + DABCO →

20 mg of **7^{Ph}** was weighed into a 20 mL scintillation vial and dissolved in 2 mL of toluene. 1 equivalent of DABCO was added. After stirring for 2 h, all volatiles were removed *in-vacuo*. Afterwards, the residual material was dissolved in C_6D_6 (**Figure S50**).

7^{Ph} + BCF→

10 mg of **7^{Ph}** was weighed into a 20 mL scintillation vial and dissolved in 500 µL of $CDCl_3$. 1 equivalent of BCF was added (**Figure S51**).

7^{Ph} + $[H(Et_2O)_2][B(C_6F_5)_4]$ →

20 mg of **7^{Ph}** was weighed into a 20 mL scintillation vial and dissolved in 4 mL of Et_2O. 1 equivalent of $[H(Et_2O)_2][B(C_6F_5)_4]$was added. The mixture was stirred for 2 h, filtered, and evaporated. The remaining material was dissolved in $CDCl_3$ (**Figure S52**).

7^{Ph} + NaO*t*Bu →

20 mg of **7^{Ph}** was weighed into a 20 mL scintillation vial and dissolved in 500 µL THF. 1 equivalent of NaO*t*Bu was added (**Figure S53**).

7^{Ph} + Verkade's Base →

20 mg of **7^{Ph}** was weighed into a 20 mL scintillation vial and dissolved in 500 µL C_6D_6. 1 equivalent of Verkade's Base was added (**Figure S54**).

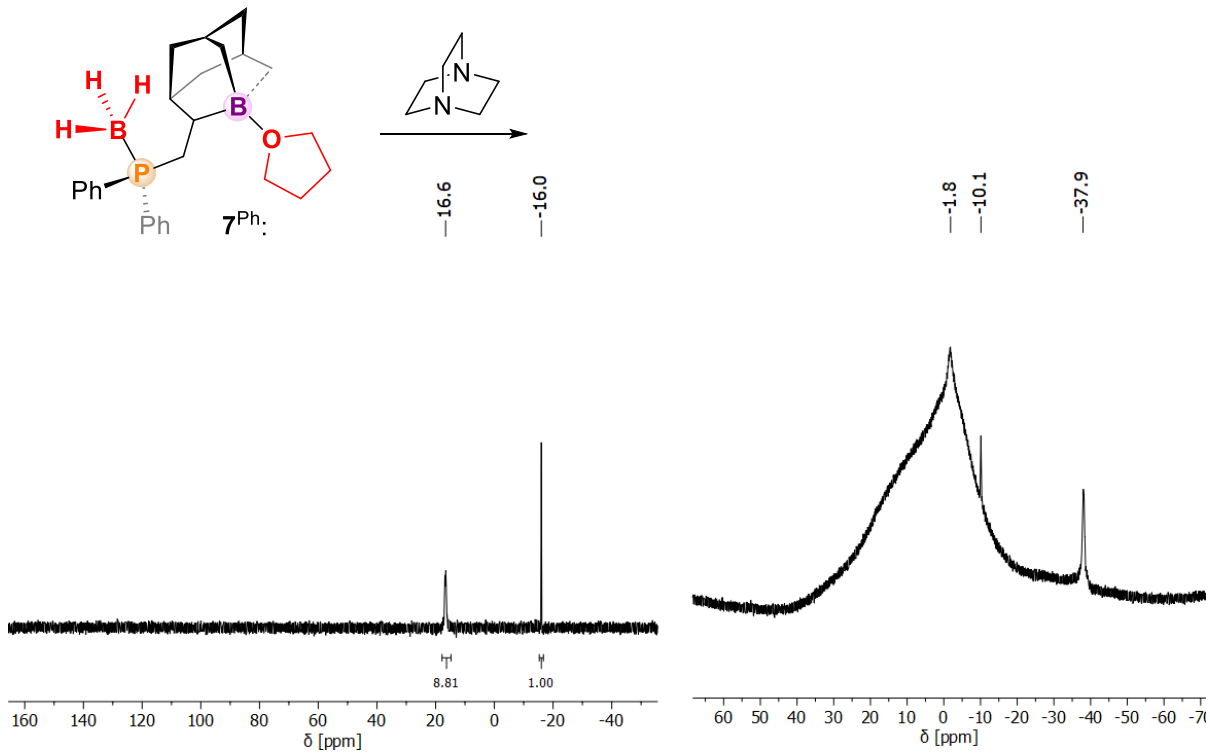

Figure S50: Reaction of 7^{Ph} with DABCO, left: $^{31}P\{^{1}H\}$ NMR, d_6-C_6D_6, 243 MHz, 298 K; right: $^{11}B\{^{1}H\}$ NMR, d_6-C_6D_6, 193 MHz, 298 K.

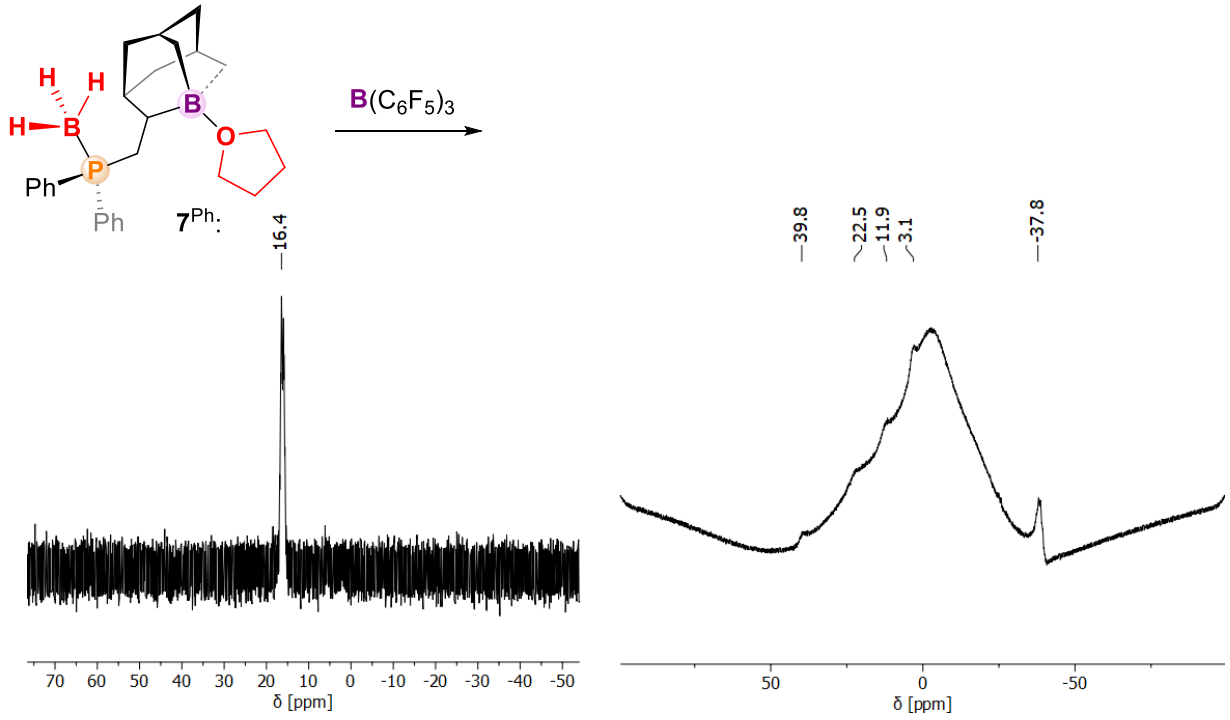

Figure S51: Reaction of 7^{Ph} with BCF, left: $^{31}P\{^{1}H\}$ NMR, d_1-$CDCl_3$, 243 MHz, 298 K; right: $^{11}B\{^{1}H\}$ NMR, d_1-$CDCl_3$, 193 MHz, 298 K.

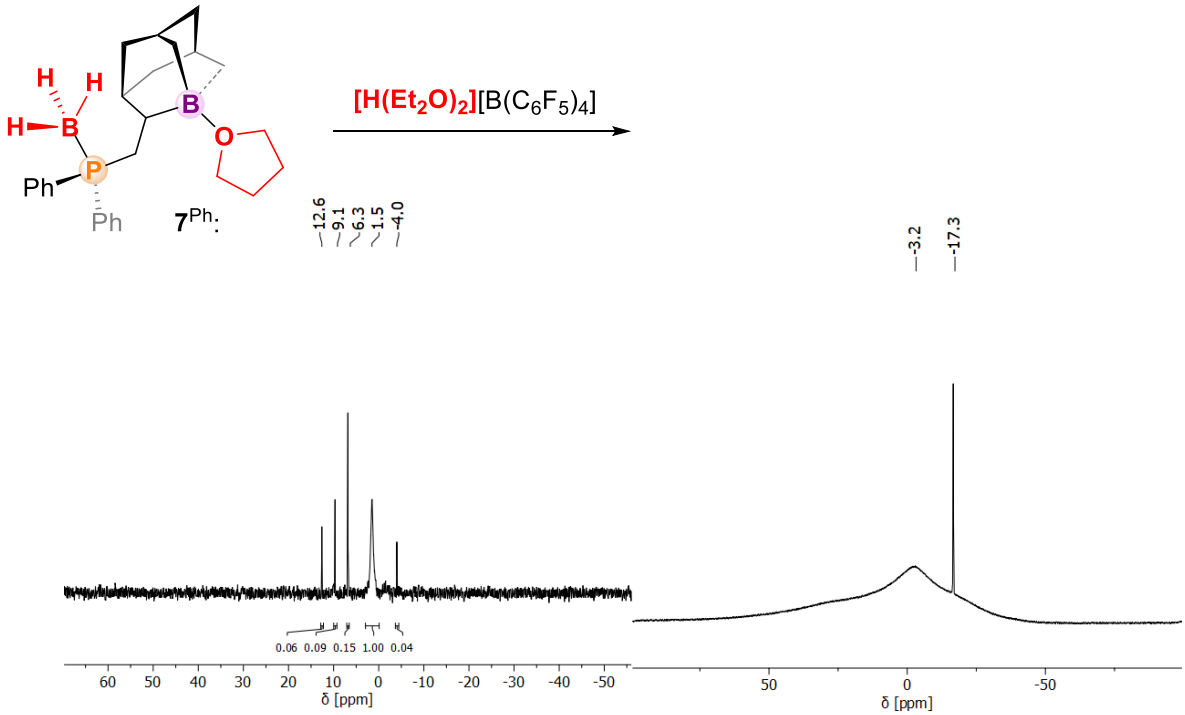

Figure S52: Reaction of 7^{Ph} with $[H(Et_2O)_2]B(C_6F_5)_4$, left: $^{31}P\{^1H\}$ NMR, d_1-$CDCl_3$, 243 MHz, 298 K; right: $^{11}B\{^1H\}$ NMR, d_1-$CDCl_3$, 193 MHz, 298 K.

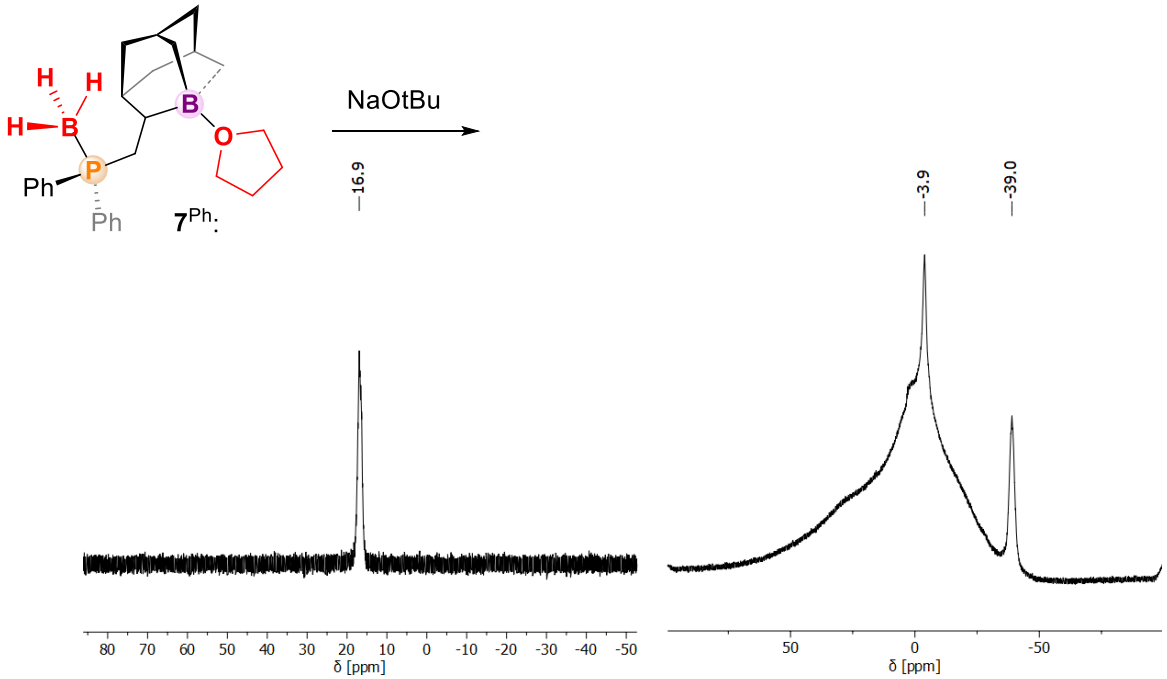

Figure S53: Reaction of 7^{Ph} with NaO*t*Bu, left: $^{31}P\{^1H\}$ NMR, THF, 243 MHz, 298 K; right: $^{11}B\{^1H\}$ NMR, THF, 193 MHz, 298 K.

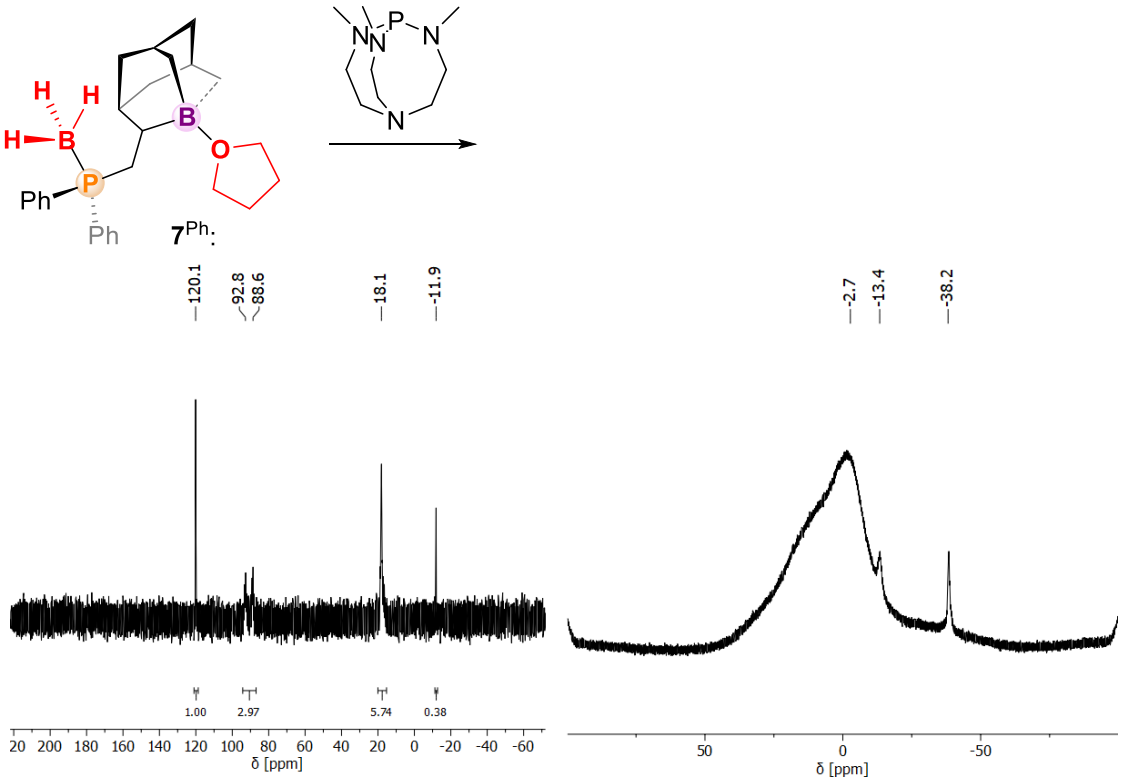

Figure S54: Reaction of 7^{Ph} with Verkade's base, left: $^{31}P\{^{1}H\}$ NMR, d_6-C_6D_6, 243 MHz, 298 K; right: $^{11}B\{^{1}H\}$ NMR, d_6-C_6D_6, 193 MHz, 298 K.

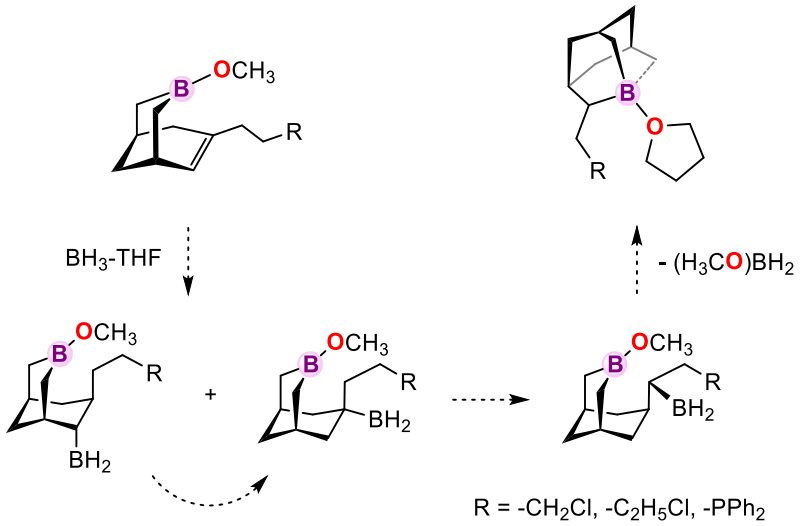

Figure S55 Proposed hydroboration-isomerization mechanism for 1-boraadamantane formation.[2]

X-Ray Crystallography:

Crystal data were collected with Mo*Kα* radiation on a Bruker Kappa Axis Apex2 diffractometer at Western University and on a Bruker VENTURE Dual Source diffractometer at McMaster University. All crystals were mounted on a MiTeGen loop with a small amount of Paratone N oil. Frame integration, scaling and absorption correction were performed using SAINT and SADABS integrated in Apex4.[3] The structures were solved with the ShelXT[4] structure solution program using intrinsic phasing and refined with the ShelXL[5] refinement package using least squares on weighted F2 values for all reflections using OLEX2.[6] CCDC **2355758**, **2355760**, **2355759**, **2355761**, **2355762**, **2355763**, **2355764**, and **2355765** contain the supplementary crystallographic data for this paper. These data are provided free of charge by The Cambridge Crystallographic Data Centre.

Table S1. Crystallographic data

	$\mathbf{2^{Ph}}$	$\mathbf{4^{Ph}}$	$\mathbf{2^{t\text{-}Bu}}$	$\mathbf{4^{t\text{-}Bu}}$	$\mathbf{7^{Ph}}$
CCDC number	2355758	2355760	2355759	2355761	2355762
empirical formula	$C_{24}H_{30}BP$	$C_{23}H_{28}BP$	$C_{20}H_{38}BP$	$C_{19}H_{36}BP$	$C_{26}H_{37}B_2OP$
formula weight	360.26	346.23	320.28	306.26	418.14
temperature [K]	100.0	100.00	110.15	100.00	100.00
crystal system	triclinic	orthorhombic	monoclinic	orthorhombic	triclinic
space group	*P*-1	$P2_12_12_1$	$P2_1/c$	*Pbca*	*P*-1
a [Å]	9.6433(4)	7.1446(8)	13.620(8)	15.2898(7)	9.1755(6)
b [Å]	10.8253(5)	12.0021(13)	10.375(6)	12.3183(5)	11.3395(7)
c [Å]	10.9474(5)	21.825(2)	13.264(7)	19.1817(8)	12.5538(8)
α [°]	75.970(2)	90	90	90	78.769(2)
β [°]	65.639(2)	90	93.932(13)	90	77.719(3)
γ [°]	70.947(2)	90	90	90	67.258(2)
volume [Å^3]	976.29(8)	1871.5(4)	1869.9(19)	3612.8(3)	1167.84(13)
Z	2	4	4	8	2
ρ_{calcd} [g · cm^{-3}]	1.225	1.229	1.138	1.126	1.189
μ [mm^{-1}]	0.146	0.149	0.143	0.146	0.133
F(000)	388.0	744.0	712.0	1360.0	452.0
dimension [mm]	0.323 × 0.209 × 0.172	0.475 × 0.122 × 0.093	0.34 × 0.322 × 0.075	0.394 × 0.305 × 0.22	0.404 × 0.24 × 0.148
radiation	MoKα (λ = 0.71073)	MoKα (λ = 0.71073)	MoKα (λ = 0.71073)	MoKα (λ = 0.71073)	MoKα (λ = 0.71073)
2Θ range for data collection/°	5.06 to 56.684	3.872 to 52.818	6.662 to 72.786	4.748 to 52.776	3.926 to 56.654
index ranges	-12 ≤ h ≤ 12, -14 ≤ k ≤ 14, -14 ≤ l ≤ 14	-5 ≤ h ≤ 8, -13 ≤ k ≤ 15, -27 ≤ l ≤ 27	-22 ≤ h ≤ 22, -17 ≤ k ≤ 17, -22 ≤ l ≤ 22	-19 ≤ h ≤ 18, -11 ≤ k ≤ 15, -23 ≤ l ≤ 23	-12 ≤ h ≤ 12, -15 ≤ k ≤ 15, -16 ≤ l ≤ 16
reflections collected	39925	13486	117764	37409	44609
independent reflections	4846 [R_{int} = 0.0351, R_{sigma} = 0.0198]	3708 [R_{int} = 0.0512, R_{sigma} = 0.0608]	9085 [R_{int} = 0.0689, R_{sigma} = 0.0332]	3683 [R_{int} = 0.0436, R_{sigma} = 0.0223]	5809 [R_{int} = 0.0389, R_{sigma} = 0.0232]
data/restraints/parameters	4846/0/235	3708/156/308	9085/0/351	3683/0/196	5809/0/283
goodness-of-fit on F^2	1.046	1.053	1.039	1.034	1.041
final *R* indexes [$I > 2\sigma(I)$]	R_1 = 0.0324, wR_2 = 0.0857	R_1 = 0.0440, wR_2 = 0.0855	R_1 = 0.0364, wR_2 = 0.0877	R_1 = 0.0462, wR_2 = 0.1178	R_1 = 0.0376, wR_2 = 0.0975
final *R* indexes [all data]	R_1 = 0.0345, wR_2 = 0.0875	R_1 = 0.0637, wR_2 = 0.0932	R_1 = 0.0558, wR_2 = 0.0973	R_1 = 0.0485, wR_2 = 0.1203	R_1 = 0.0428, wR_2 = 0.1013
largest diff. peak/hole [e Å^{-3}]	0.35/-0.25	0.21/-0.33	0.42/-0.24	0.56/-0.39	0.41/-0.20

	8$^{t\text{-Bu}}$-DMAP	**9$^{t\text{-Bu}}$**	**10$^{t\text{-Bu}}$**
CCDC number	2355763	2355764	2355765
empirical formula	$C_{26}H_{46}BN_2P$	$C_{29}H_{53.5}AuBClN_2O_{0.75}P$	$C_{56}H_{102}B_2N_4O_{0.5}P_2Pt$
formula weight	428.43	716.43	1118.06
temperature [K]	110.00	110	110
crystal system	triclinic	triclinic	triclinic
space group	*P*-1	*P*-1	*P*-1
a [Å]	11.1805(5)	7.1927(4)	10.6781(5)
b [Å]	11.2066(5)	11.9175(6)	10.9251(5)
c [Å]	11.5832(5)	19.1310(10)	12.9656(6)
α [°]	69.782(2)	78.6195(18)	101.270(3)
β [°]	80.362(2)	86.0612(18)	98.789(3)
γ [°]	74.668(2)	86.5573(18)	90.250(3)
volume [Å^3]	1308.78(10)	1602.04(15)	1465.06(12)
Z	2	2	1
ρ_{calcd} [g · cm^{-3}]	1.087	1.485	1.267
μ [mm^{-1}]	0.120	4.747	2.487
F(000)	472.0	727.0	588.0
dimension [mm]	0.24 × 0.13 × 0.102	0.387 × 0.122 × 0.072	0.187 × 0.117 × 0.117
radiation	MoKα (λ = 0.71073)	MoKα (λ = 0.71073)	MoKα (λ = 0.71073)
2Θ range for data collection/°	3.76 to 52.812	2.176 to 61.286	6.158 to 51.658
index ranges	-13 ≤ h ≤ 13, -14 ≤ k ≤ 14, -14 ≤ l ≤ 14	-10 ≤ h ≤ 10, -17 ≤ k ≤ 17, -27 ≤ l ≤ 27	-13 ≤ h ≤ 13, -13 ≤ k ≤ 13, -15 ≤ l ≤ 15
reflections collected	88793	100956	91063
independent reflections	5354 [R_{int} = 0.0608, R_{sigma} = 0.0212]	9843 [R_{int} = 0.0685, R_{sigma} = 0.0344]	5569 [R_{int} = 0.0900, R_{sigma} = 0.0338]
data/restraints/parameters	5354/0/279	9843/67/391	5569/40/340
goodness-of-fit on F^2	1.047	1.040	1.053
final *R* indexes [$I > 2\sigma(I)$]	R_1 = 0.0389, wR_2 = 0.0985	R_1 = 0.0314, wR_2 = 0.0630	R_1 = 0.0371, wR_2 = 0.0924
final *R* indexes [all data]	R_1 = 0.0483, wR_2 = 0.1065	R_1 = 0.0406, wR_2 = 0.0660	R_1 = 0.0375, wR_2 = 0.0927
largest diff. peak/hole [e Å^{-3}]	0.35/-0.30	2.31/-2.12	1.35/-2.29

$$R1 = \Sigma \, ||F_o| - |F_c|| \, / \, \Sigma \, |F_o| ; \; wR2 = [\Sigma(w(F_o^2 - F_c^2)^2) \, / \, \Sigma \, w(F_o^2)^2]^{1/2}$$

Computational Details:

All calculations were performed using version 5.0.3 of the ORCA computational package[7] and were run on the Graham cluster maintained by Compute Canada. All geometry optimizations and frequency calculations were performed at the B3LYP-D3(BJ)/def2-TZVPP level of theory.[8] The RIJCOSX approximation was used to enhance computational efficiency, along with the auxiliary basis *def2/J*.[9] Convergence criteria were met using the *defgrid2* integral grid size. Frequency calculations (*Freq*) were performed to confirm that each optimized geometry was a true minimum indicated by the absence of imaginary frequencies. Single-point calculations were performed at the B3LYP-D3(BJ)/def2-TZVPP level of theory on optimized geometries. For selected compounds, the implicit solvation model CPCM (as integrated in ORCA) was applied with a dielectric constant of $\varepsilon = 4.9$ (corresponds to CH_2Cl_2).[10]

Table S2. Energetic data calculated at B3LYP-D3(BJ)/def2-TZVPP level of theory.

Compound	Total thermal energy in E_h	Total Enthalpy in E_h	Gibbs Free Energy at 298.15 K in E_h
2^{Ph} open	-1298.132375	-1298.131431	-1298.20445
4^{Ph} open	-1258.858898	-1258.857954	-1258.927612
7^{Ph} open	-1219.591419	-1219.590475	-1219.656709
2^{Ph} closed	-1298.163381	-1298.162437	-1298.231912
4^{Ph} closed	-1258.887342	-1258.886398	-1258.953857
7^{Ph} closed	-1219.583492	-1219.582548	-1219.648487
$2^{t\text{-}Bu}$ open	-1150.474777	-1150.473832	-1150.548461
$4^{t\text{-}Bu}$ open	-1111.200382	-1111.199438	-1111.270964
$7^{t\text{-}Bu}$ open	-1071.926218	-1071.925274	-1071.993516
$2^{t\text{-}Bu}$ closed	-1150.510798	-1150.509854	-1150.579224
$4^{t\text{-}Bu}$ closed	-1111.230386	-1111.229442	-1111.297579
$7^{t\text{-}Bu}$ closed	-1071.922716	-1071.921772	-1071.988395
BH_3-THF	-258.8931223	-258.8921781	-258.9302425
7^{Ph} + BH_3-THF	-1478.536015	-1478.535071	-1478.616828
$7^{t\text{-}Bu}$ + BH_3-THF	-1330.8777	-1330.876756	-1330.958927
CO_2	-188.57469	-188.5737459	-188.5979947
4^{Ph} + CO_2	-1447.438927	-1447.437982	-1447.511893
7^{Ph} + CO_2	-1408.175597	-1408.174653	-1408.245796
$4^{t\text{-}Bu}$ + CO_2	-1299.788251	-1299.787306	-1299.862082
$7^{t\text{-}Bu}$ + CO_2	-1260.528063	-1260.527119	-1260.598778
H_2	-1.1611087	-1.16016449	-1.17495694
4^{Ph} + H_2	-1260.004628	-1260.003684	-1260.072158
7^{Ph} + H_2	-1220.734008	-1220.733064	-1220.799286
$4^{t\text{-}Bu}$ + H_2	-1112.355965	-1112.35502	-1112.424591
$7^{t\text{-}Bu}$ + H_2	-1073.080941	-1073.079997	-1073.147424

BAd	-376.5394094	-376.5384651	-376.577854
PPh_2Me	-844.2242627	-844.2233185	-844.2754205
PPh_2Et	-883.4975519	-883.4966076	-883.5521933
PPh_2Pr	-922.7725947	-922.7716505	-922.8296257
P*t*-Bu_2Me	-696.5688826	-696.5679384	-696.6206629
P*t*-Bu_2Et	-735.8384761	-735.8375319	-735.8930923
P*t*-Bu_2Pr	-775.1130585	-775.1121143	-775.1704333
BAd + PPh_2Me	-1220.802699	-1220.801755	-1220.87029
BAd + PPh_2Et	-1260.076332	-1260.075388	-1260.146689
BAd + PPh_2Pr	-1299.350284	-1299.349339	-1299.42256
BAd + P*t*-Bu_2Me	-1073.144962	-1073.144017	-1073.21247
BAd + P*t*-Bu_2Et	-1112.413016	-1112.412072	-1112.483126
BAd + P*t*-Bu_2Pr	-1151.68855	-1151.687606	-1151.761541

Table S3. Energetic data for solvated molecules calculated at B3LYP-D3(BJ)/def2-TZVPP level of theory with implicit solvation model (CPCM, ε = 4.9).

Compound	Total thermal energy in E_h	Total Enthalpy in E_h	Gibbs Free Energy at 298.15 K in E_h
7^{Ph} open	-1219.599689	-1219.598745	-1219.665123
4^{Ph} closed	-1258.896981	-1258.896037	-1258.963582
$7^{t\text{-}Bu}$ open	-1071.932428	-1071.931484	-1071.999741
$4^{t\text{-}Bu}$ closed	-1111.23753	-1111.236586	-1111.304907
CO_2	-188.57746	-188.5765138	-188.6007714
4^{Ph} + CO_2	-1447.462472	-1447.461527	-1447.534717
7^{Ph} + CO_2	-1408.196604	-1408.19566	-1408.266961
$4^{t\text{-}Bu}$ + CO_2	-1299.808968	-1299.808024	-1299.882916
$7^{t\text{-}Bu}$ + CO_2	-1260.54783	-1260.546886	-1260.61858
H_2	-1.16143601	-1.1604918	-1.17528635
4^{Ph} + H_2	-1260.017714	-1260.01677	-1260.087252
7^{Ph} + H_2	-1220.747824	-1220.746879	-1220.814944
$4^{t\text{-}Bu}$ + H_2	-1112.370605	-1112.369661	-1112.441758
$7^{t\text{-}Bu}$ + H_2	-1073.099418	-1073.098474	-1073.16693

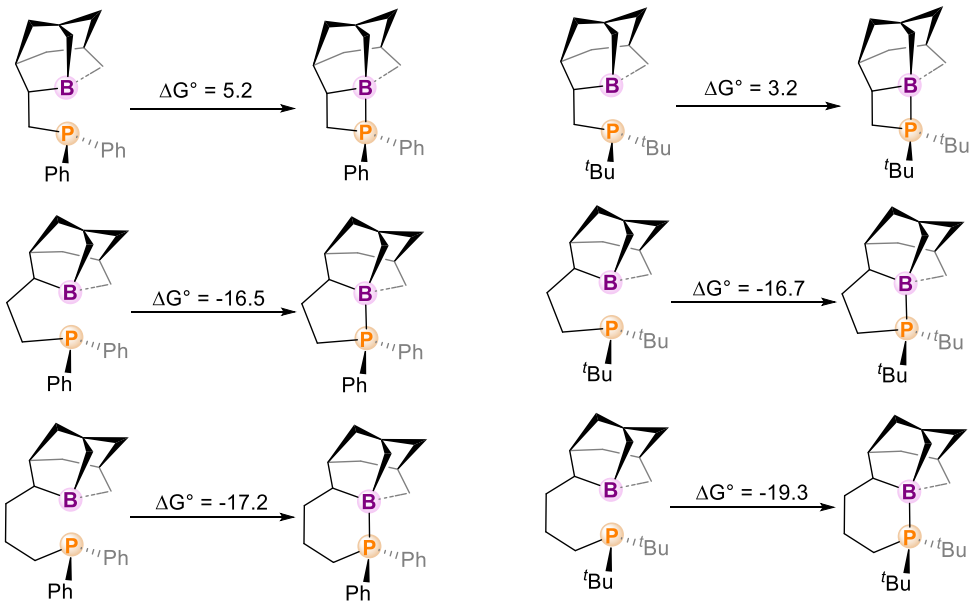

Figure S56 Comparison of Gibbs free energies ΔG° in the gas-phase for ring closure reactions of C1, C2 and C3 linked 2-alkylphosphino-1-boraadamantanes. Energies are given in kcal mol^{-1}.

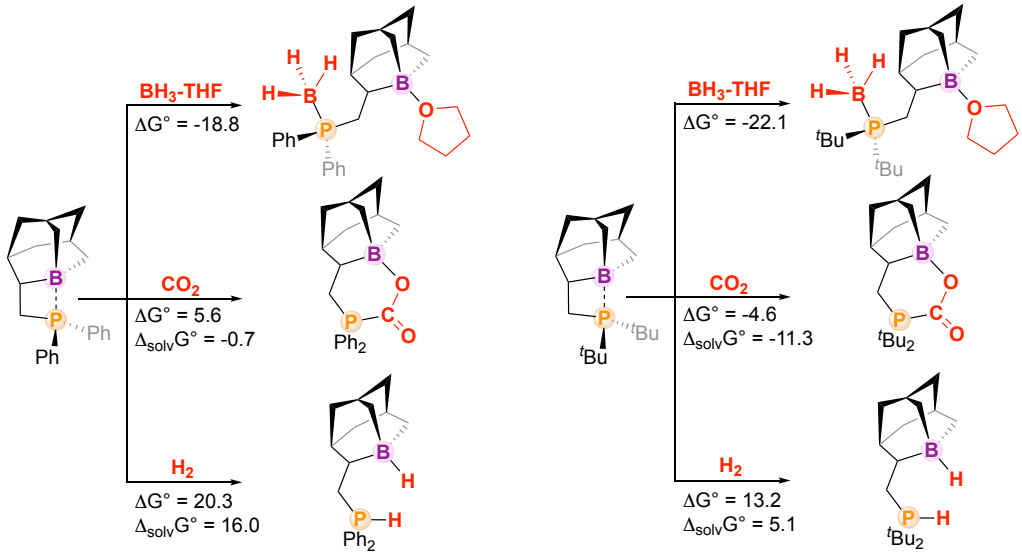

Figure S57 Comparison of Gibbs free energies in the gas-phase ΔG° and with implicit solvent model (CH_2Cl_2) $\Delta_{solv}G°$ for reactions of **7^{Ph}** and **7$^{t\text{-}Bu}$** with BH_3-THF, CO_2 and H_2. Energies are given in kcal mol^{-1}.

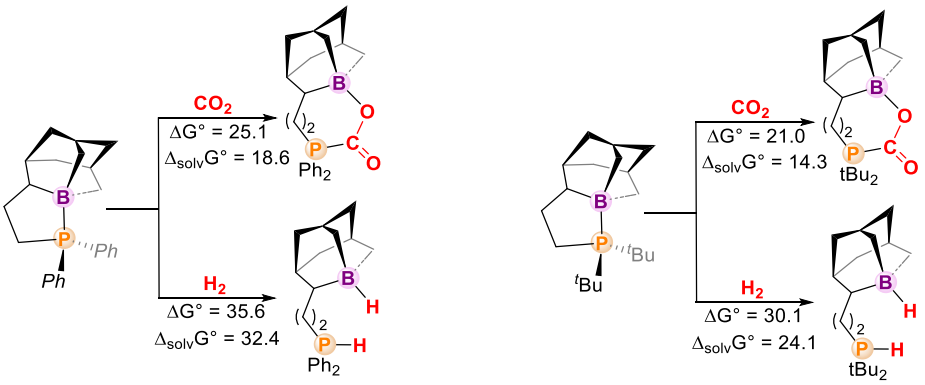

Figure S58 Comparison of Gibbs free energies in the gas-phase ΔG° and with implicit solvent model (CH_2Cl_2) $\Delta_{solv}G°$ for reactions of $\mathbf{4^{Ph}}$ and $\mathbf{4^{t\text{-}Bu}}$ with CO_2 and H_2. Energies are given in kcal mol^{-1}.

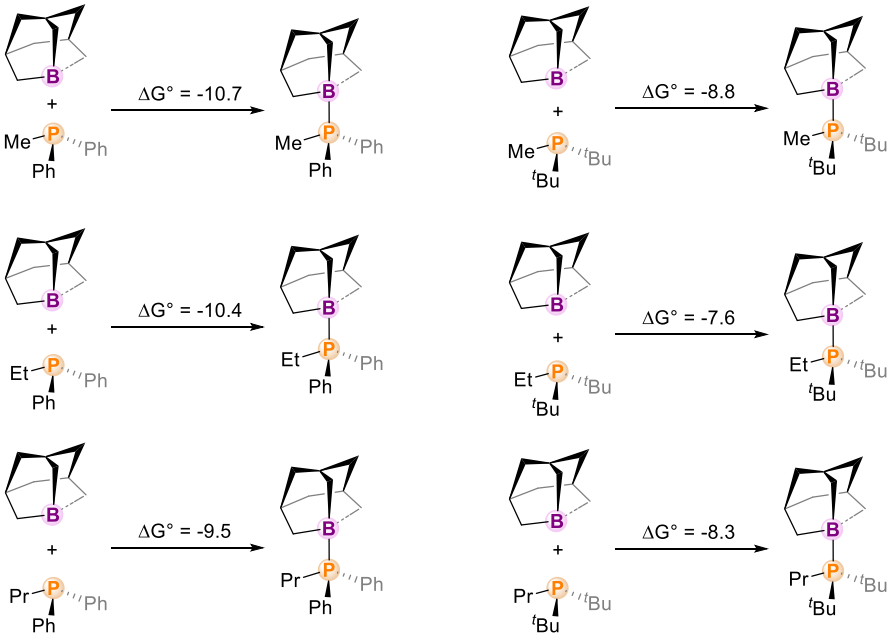

Figure S59 Comparison of Gibbs free energies ΔG° in the gas-phase for adduct formation of 1-boraadamantane and different-alkylphosphines. Energies are given in kcal mol^{-1}.

Determination of the percent buried volume of $8^{t\text{-Bu}}$

The values were calculated from the molecular structures of gold complex $\mathbf{9}^{t\text{-Bu}}$ by using ***SambVca 2.1.***[11] Hereby, the Au-P distances was set to 2.28 Å, Bondi radii scaled by 1.17, sphere radius set to 3.5, hydrogen atoms were omitted.

Table S4. Calculated percent buried volumes $\%V_{bur}$ for selected phosphines.

Phosphine	**$\%V_{bur}$**
PPh_3	30.0[12]
PCy_3	33.2[12]
$P(t\text{-Bu})_3$	38.0[12]
$8^{t\text{-Bu}}$-DMAP	38.7
$P(o\text{-tol})_3$	39.4[13]
$PMes_3$	45.0[13]

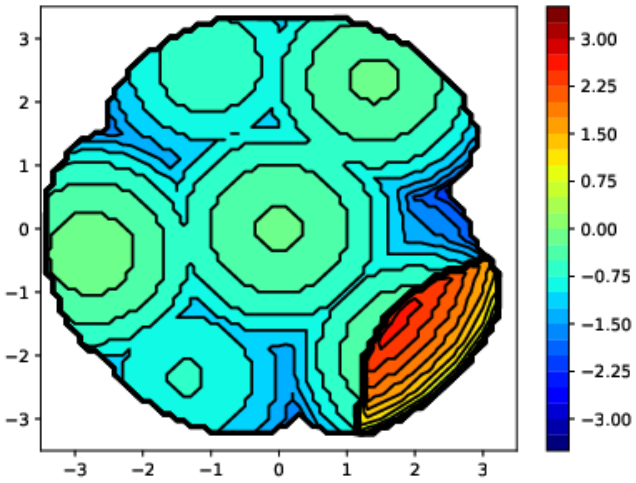

Figure S60 Steric map for the depiction of $\%V_{bur}$ for ligand $\mathbf{8}^{t\text{-Bu}}$**.**

References:

[1] a) Y.N. Bubnov, T. V. Potapova, M. E. Gursky, *J. Organomet. Chem.* **1991**, *412*, 311; b) Y. Huang, Le Zhang, W. Wei, F. Alam, T. Jiang, *Phosphorus Sulfur* **2018**, *193*, 363; c) J. Meiners, A. Friedrich, E. Herdtweck, S. Schneider, *Organometallics* **2009**, *28*, 6331.

[2] M. E. Gurskii, S. Y. Erdyakov, T. V. Potapova, Y. N. Bubnov, *Russ Chem Bull* **2008**, *57*, 802.

[3] Bruker, *Apex4, SAINT, and SADABS.*, Bruker AXS Inc, Madison, Wisconsin, USA., **2021**.

[4] G. M. Sheldrick, *Acta Crystallogr. A* **2015**, *71*, 3.

[5] G. M. Sheldrick, *Acta Crystallogr. C* **2015**, *71*, 3.

[6] O. V. Dolomanov, L. J. Bourhis, R. J. Gildea, J. A. K. Howard, H. Puschmann, *J. Appl. Crystallogr.* **2009**, *42*, 339.

[7] F. Neese, *WIREs Comput Mol Sci* **2022**, *12*, 12753.

[8] a) S. Grimme, J. Antony, S. Ehrlich, H. Krieg, *J. Chem. Phys.* **2010**, *132*, 154104; b) S. Grimme, S. Ehrlich, L. Goerigk, *J. Comput. Chem.* **2011**, *32*, 1456; c) F. Weigend, R. Ahlrichs, *Phys. Chem. Chem. Phys.* **2005**, *7*, 3297.

[9] F. Weigend, *Phys. Chem. Chem. Phys.* **2006**, *8*, 1057.

[10] V. Barone, M. Cossi, *J. Phys. Chem. A* **1998**, *102*, 1995.

[11] L. Falivene, Z. Cao, A. Petta, L. Serra, A. Poater, R. Oliva, V. Scarano, L. Cavallo, *Nat. Chem.* **2019**, *11*, 872.

[12] J. A. Werra, K. Wurst, L. B. Wilm, P. Löwe, M. B. Röthel, F. Dielmann, *Organometallics* **2023**, *42*, 597.

[13] H. Clavier, S. P. Nolan, *Chem. Commun.* **2010**, *46*, 841.